NAVAL POSTGRADUATE SCHOOL
MONTEREY, CALIFORNIA

THESIS

FINITE ELEMENT MODELING OF SANDWICH COMPOSITE STRUCTURES SUBJECT TO LOW VELOCITY IMPACT AND DELAMINATION

by

Gerald W. Wojcik

December, 1995

Thesis Advisor: Young W. Kwon

Approved for public release; distribution is unlimited.

19960402 119

1. AGENCY USE ONLY *(Leave blank)*	2. REPORT DATE December 1995	3. REPORT TYPE AND DATES COVERED Master's Thesis	
4. TITLE AND SUBTITLE FINITE ELEMENT MODELING OF SANDWICH COMPOSITE STRUCTURES SUBJECT TO LOW VELOCITY IMPACT AND DELAMINATION		5. FUNDING NUMBERS	
6. AUTHOR(S) Wojcik, Gerald W.			
7. PERFORMING ORGANIZATION NAME(S) AND ADDRESS(ES) Naval Postgraduate School Monterey CA 93943-5000		8. PERFORMING ORGANIZATION REPORT NUMBER	
9. SPONSORING/MONITORING AGENCY NAME(S) AND ADDRESS(ES)		10. SPONSORING/MONITORING AGENCY REPORT NUMBER	

11. SUPPLEMENTARY NOTES The views expressed in this thesis are those of the author and do not reflect the official policy or position of the Department of Defense or the U.S. Government.

12a. DISTRIBUTION/AVAILABILITY STATEMENT Approved for public release; distribution is unlimited.	12b. DISTRIBUTION CODE

13. ABSTRACT

Two common concerns in the use of sandwich composite construction are the effects of low velocity impact and delamination upon structural failure. Finite element analysis of these events can provide a comprehensive time history of the resulting stress, strain, displacement, and velocity at all points in a structure. The purpose of this research is to develop a finite element model of a sandwich composite and use this model to analyze the dynamic response of an unbalanced sandwich beam, a balanced sandwich beam, and a balanced sandwich plate subject to low velocity impact. In particular, strain vs. time history, failure location and mode, and the influence of an existing delamination are investigated. It is found that, in the presence of a small delamination, the failure load of a sandwich composite structure increases. Also, failure in general is due to asymetric core shear and the location of this failure shifts to the delamination boundry in the case of a large delamination. Finally, it is noted that detecting the presence of a delamination using maximum displacement values may be difficult.

14. SUBJECT TERMS sandwich composite, low velocity impact, delamination			15. NUMBER OF PAGES 102
			16. PRICE CODE
17. SECURITY CLASSIFICATION OF REPORT Unclassified	18. SECURITY CLASSIFICATION OF THIS PAGE Unclassified	19. SECURITY CLASSIFICATION OF ABSTRACT Unclassified	20. LIMITATION OF ABSTRACT UL

FINITE ELEMENT MODELING OF SANDWICH COMPOSITE STRUCTURES SUBJECT TO LOW VELOCITY IMPACT AND DELAMINATION

Gerald W. Wojcik
Lieutenant Commander, United States Navy
B.S., University of Pittsburgh at Johnstown, 1981

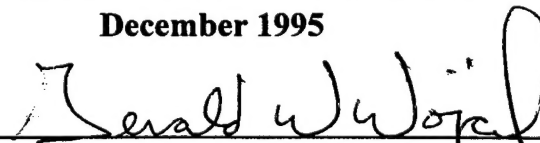Submitted in partial fulfillment
of the requirements for the degree of

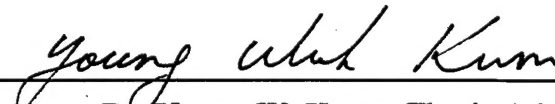**MASTER OF SCIENCE IN MECHANICAL ENGINEERING**
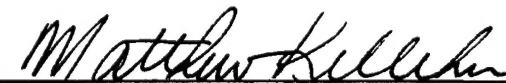
from the

NAVAL POSTGRADUATE SCHOOL
December 1995

Author: _____
Gerald W. Wojcik

Approved by: _____
Dr. Young W. Kwon, Thesis Advisor

_____
Matthew D. Kelleher, Chairman
Department of Mechanical Engineering

iii

ABSTRACT

Two common concerns in the use of sandwich composite construction are the effects of low velocity impact and delamination upon structural failure. Finite element analysis of these events can provide a comprehensive time history of the resulting stress, strain, displacement, and velocity at all points in a structure. The purpose of this research is to develop a finite element model of a sandwich composite and use this model to analyze the dynamic response of an unbalanced sandwich beam, a balanced sandwich beam, and a balanced sandwich plate subject to low velocity impact. In particular, strain vs. time history, failure location and mode, and the influence of an existing delamination are investigated. It is found that, in the presence of a small delamination, the failure load of a sandwich composite structure increases. Also, failure in general is due to asymetric core shear and the location of this failure shifts to the delamination boundry in the case of a large delamination. Finally, it is noted that detecting the presence of a delamination using maximum displacement values may be difficult.

TABLE OF CONTENTS

LIST OF FIGURES

LIST OF TABLES

I. INTRODUCTION

A sandwich structure consists of a thick, lightweight core sandwiched between two thin, stiff facings. The core material is characteristically low in density, elastic modulus, and shear modulus, and is typically some form of foam or honeycomb. The facings have a high elastic strength and modulus. They may be of the same material and dimensions (balanced sandwich) or of different materials and dimensions (unbalanced sandwich).

The primary purpose of sandwich construction is to produce a stiff, yet lightweight structure. This purpose is obviously achieved by attempting to combine the desirable low density properties of the core with the high stiffness properties of the faceplates into one composite material. Other desirable characteristics of sandwich construction that may be realized are corrosion and fatigue resistance.

Sandwich construction has been incorporated into a great variety of aerospace design configurations. The first production aircraft to incorporate this construction was the British de Havilland Mosquito, a World War II high-speed, reconnaissance/bomber that utilized structures of a balsa-wood core covered by plywood facings. Since then, sandwich construction has been incorporated into the production of the B-58, B-70, and F111 series aircraft, as well as helicopter rotor blades, satellites, and other spacecraft.

Recently, the Navy conducted research and development of an Advanced Performance Mast System (APMS) for the DD963 Spruance class destroyer. This project, which was headed by the Naval Surface Warfare Center, Carderock Division, was initiated to develop a surface ship mast structure constructed entirely of composite materials which would enclose all radars, antennas and sensors.

One of the major concerns in the use of sandwich composites is the loss of load carrying ability due to a delamination between the facing and the core. A common cause of this type of delamination is low velocity impact of a foreign object upon the facing.

Several experimental studies have been conducted into the effects of low velocity impact and delamination upon sandwich composite materials. Two conducted at the Naval Postgraduate School were done by Fuller [Ref. 1] and Clawson [Ref. 2]. Fuller examined low velocity impact effects upon the APMS composite, which was an unbalanced, titanium-honeycomb-glass reinforced plastic sandwich. Clawson investigated the effects of a pre-existing delamination upon a balanced, carbon-foam sandwich subject to low velocity impact.

Experimental studies such as these are important in understanding the impact response of sandwich construction. However, they cannot provide the full picture of response. Only a finite number of gages can be put on a test specimen in a finite number of locations, and this certainly limits the total amount of data that can be obtained.

Computer modeling, on the other hand, can provide a comprehensive time history of an impact event in terms of stress, strain, displacement, velocity, or almost any other desired parameter at any point of interest in the structure. Further, computer simulation is often less complex in setup and time required (ie. less expensive).

To this end, the purpose of this research is to develop a qualitatively correct finite element model of the APMS unbalanced, sandwich composite, validate the model using Fuller's experimental results, and use the model to examine the characteristics of deflection, strain, and failure during impact. Additionally, this model is to be used as a basis to investigate and explain the failure locations and mechanisms of Clawson's experimental work. Finally, the model is used to make predictions as to the dynamic response and failure of a delaminated, carbon-foam sandwich plate. The effect of friction in the delamination area and the possibility of determining the presence of a delamination based upon deflection response are also examined.

II. BACKGROUND

A. COMPARISON OF SANDWICH BEAM ANALYSIS TO CLASSICAL BEAM THEORY

A sandwich composite is analogous in many respects to a structural I-beam, with the faceplates representing the beam flanges and the core representing the beam web. The core separates the faceplates so that they are sufficiently spaced to increase the bending rigidity.

In general, the core will have a bending modulus very small with respect to the faces. Therefore, it carries essentially no bending load, leaving all bending stresses to be supported by the faceplates.

In an unbalanced sandwich, the neutral axis of the beam is not at the plate's centerline. Therefore, the beam's faces are not equidistant from the neutral axis. This implies that the bending stress experienced by the two faces in a static, three point bending configuration will be different.

Where the sandwich beam differs from the I-beam in a flexural analysis is the existence of transverse shear and through-thickness deformations in the core. In classical beam theory, these deformations are neglected. However, in a sandwich beam, they may be significant.

B. LITERATURE SURVEY

Reviewing the literature, it was found that much research has been conducted into the areas of low velocity impact and delamination of laminated composite materials. However, very little work has been done in these areas concerning sandwich composites. Additionally, it appears that almost no research has been published pertaining to unbalanced, sandwich composites.

Nemes and Simmonds [Ref. 3] conducted a computational and experimental investigation of the low velocity impact response of a balanced sandwich plate with GRP faceplates and a foam core. The methodology utilized for predicting response was based

3

on a knowledge of the constitutive behavior of each of the sandwich components (core, faceplate, and bond layers). It was found that, during impact, the portion of total deformation due to transverse shear deformation was significant. Additionally, comparing the strain history of the non-impacted surface with its displacement history, it was noted that, when the strain returned to zero, the plate was still deformed. This was due to the effect of shear deformation in the core, a portion of which is either slowly recoverable or non-recoverable.

Lee, Huang, and Fann [Ref. 4] performed an experimental and analytical analysis of a balanced sandwich plate consisting of graphite/epoxy faceplates and a polyurethane foam core being impacted by a rigid ball. They found that the core transmits both transverse shear and transverse normal (through-thickness) deformations. From this observation, it was noted that the impacted and non-impacted surfaces of the plate deformed differently. Additionally, it was found that both the impact velocity and the impactor's mass affected the magnitude of the contact force between the plate and the ball, with the impact velocity being the more significant factor.

Sjoblom, Hartness, and Cordell [Ref. 5] investigated low velocity impact testing of composite materials in general. They found that the energy lost during impact was a more direct measure of damage than the actual impact energy. From this observation, it was concluded that both the impact and rebound velocities were required to be measured accurately. Also, it was found that a static test can give very similar results to a low velocity impact test if the material is not strain-rate sensitive. This characteristic was based on neglecting the inertial forces of the structure.

Wu and Shyu [Ref. 6] performed an experimental study of the contact (static) and low velocity impact responses of composite laminates impacted by rigid spheres. As did Sjoblom, Hartness, and Cordell, they found that the responses to the quasi-static contact and low velocity impact tests were very similar.

4

C. SUMMARY OF FULLER'S WORK

The composite configuration investigated by Fuller was an unbalanced sandwich consisting of Titanium 6A1-4V and glass reinforced plastic (GRP) faces and a phenolic, Nomex fiber reinforced honeycomb core. Low velocity impact was modeled with a simple drop weight configuration in which a free falling weight struck a simply supported, 0.3048 m (12 in), sandwich beam. The material properties of the test beam are listed in Table I for the axis orientation specified in Figure 1. (This axis orientation is utilized throughout this paper.)

Using strain gages mounted on the beam, strain vs. time data was obtained for both the impacted and bottom surfaces at the quarter points and the centerline on the bottom surface. (Strain gage locations and numbering scheme are specified in Figure 2.) Additionally, impactor displacement vs. time and velocity vs. time results were calculated using data supplied by a force transducer mounted on the drop weight. All of this information was collected for both GRP and Titanium side impacts.

Impactor drop height was varied. At a threshold value of this drop height, beam failure was noted to occur in the core material in the quarter area. (The quarter area is defined as the general length between the beam support and center line.) The mode of failure was always core crimping/shearing. Additionally, the failure was never symmetric. Shearing always occurred in one quarter area only.

5

Table I. Unbalanced Sandwich Beam Material Properties

	Titanium (Isotropic)	GRP	Hexcel-10 Core
E_x (Gpa) (psi)	113.8 (16.5×10^6)	17.24 (2.5×10^6)	0.0690 (1.0×10^4) (estimate)
E_y (Gpa) (psi)		17.24 (2.5×10^6)	0.0690 (1.0×10^4) (estimate)
E_z (Gpa) (psi)		6.895 (1.0×10^6)	0.1931 (2.8×10^4)
G_{xy} (Gpa) (psi)	39.78 (5.77×10^6)	2.965 (4.3×10^5)	0.0690 (1.0×10^4) (estimate)
G_{yz} (Gpa) (psi)		2.620 (3.8×10^5)	0.05930 (8.6×10^3)
G_{xz} (Gpa) (psi)		2.620 (3.8×10^5)	0.03241 (4.7×10^3)
ν_{xy}	0.342	0.121	0
ν_{yz}		0.044	0
ν_{xz}		0.044	0
ρ (kg/m³) (lb$_m$/in³)	4738 (0.171)	1898 (0.0685)	64.28 (0.00232)
Thickness (m) (in)	0.00254 (0.1)	0.002032 (0.08)	0.0254 (1.0)
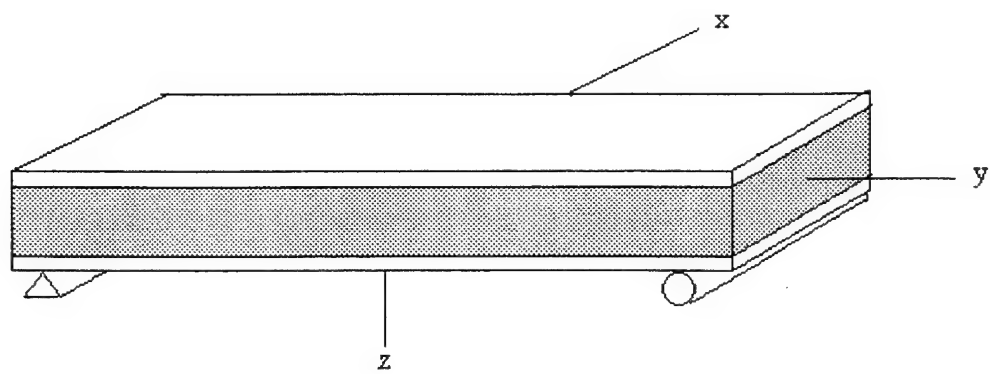
Figure 1. Axis Orientation After Ref [1].

Impacted Side   Non-impacted Side
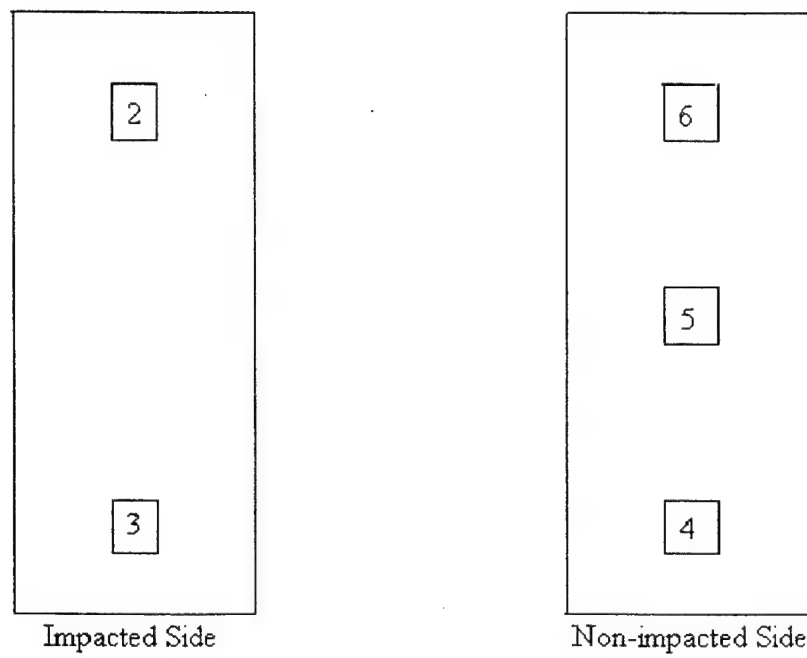
Figure 2. Strain Gage Locations and Numbering

D. SUMMARY OF CLAWSON'S WORK

The composite structure investigated by Clawson was a balanced sandwich consisting of graphite epoxy $(0_2/90_2/0_2)$ facesheets and a Rohacell Polymethacrylimide rigid foam core. Material properties are listed in Table II.

As in Fuller's work, low velocity impact was modeled using a drop weight configuration. The energy of impact was varied by incrementally adjusting the drop height. The test beam length was 0.381 m (15 in.) and the core thickness was varied. Samples were instrumented in a similar manner to Fuller's.

Samples having various lengths of delamination between the facesheet and core were tested. As anticipated, it was found that, in general, the larger the delamination size, the smaller the energy absorbed prior to failure. However, one key finding of this research was that, for a sample with a small delamination (0.0127 m or 0.5 in) impacted on the non-delaminated side, the energy absorbed by the beam prior to failure was actually higher than in the non-delaminated case.

Table II. Balanced Sandwich Beam Material Properties

	Graphite	Foam (Isotropic)
E_x (Gpa) (psi)	52.91 (7.673x10^6)	0.1565 (2.27x10^4)
E_y (Gpa) (psi)	26.48 (3.84x10^6)	
E_z (Gpa) (psi)	1.379 (2.0x10^5) (estimate)	
G_{xy} (Gpa) (psi)	13.79 (2.0x10^6)	
G_{yz} (Gpa) (psi)	3.448 (0.5x10^6) (estimate)	
G_{xz} (Gpa) (psi)	3.448 (0.5x10^6) (estimate)	
ν_{xy}	0.74	0.38
ν_{yz}	0.74 (estimate)	
ν_{xz}	0.74 (estimate)	
ρ (kg/m^3) (lb$_m$/in^3)	1302 (0.04699)	75.0 (0.002707)
Thickness (m) (in)	0.001087 (0.0428)	0.00635 (0.25)

9

III. FEM MODELS

The goal in numerical modeling was to develop a qualitatively correct simulation of the experimental, dynamic response in order to further understand the failure modes caused by mechanical impact. The modeling approach was similar to that adopted by Nemes and Simmonds [Ref. 3]. Specifically, a knowledge of the material properties of each of the sandwich components was used to predict the overall response of the composite.

All finite element meshes were developed using 8 node solid elements, and, for each case, the bond layer between the facesheet and the core was neglected. All analysis were run on a HP Series 735 computer using the contact-impact algorithm of the VEC/DYNA3D (non-linear dynamic analysis of structures in three dimensions) program.

A. UNBALANCED TI-HONEYCOMB-GRP SANDWICH BEAM

1. Model Description

The sandwich was modeled as a 0.2794 m (11 in.), simply supported, composite beam. This span was utilized due to the fact that, in Fuller's experimental work, the supports were placed 0.0127 m (0.5 in.) from the beam ends.

The finite element mesh consisted of two elements through thickness for each of the faceplates and six elements through thickness for the core. Forty longitudinal elements and two transverse elements were utilized (See Figure 3).

The impactor was modeled as a rigid, rectangular block with a 0.01524 m (0.6 in.) width to equal that of the brass plate load distributor used by Fuller. Height and weight were 0.254 m (10.0 in.) and 556.0N (125 lb_f), respectively. It was positioned 0.000254 m (0.01in.) above the sandwich beam, subjected to gravitational force, and given an initial velocity equal to that of a 0.0254 m (1.0 in) free-fall.

2. Material Property Parametric Study

The significant features of a sandwich beam's dynamic response are a function of the specific material properties of the individual sandwich components. Since
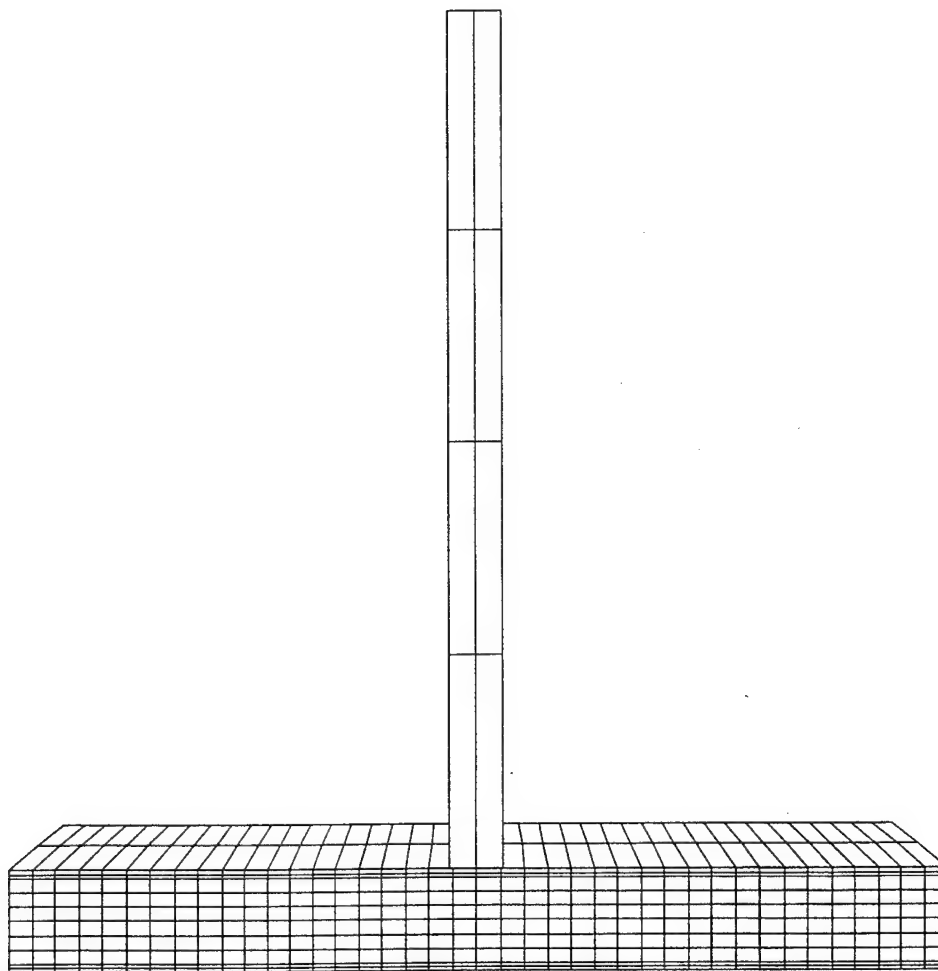
11

Figure 3. FEM Mesh of Unbalanced Ti-Honeycomb-GRP Sandwich Beam

experimental strain-time data had already been collected, a parametric study was conducted to identify those specific components and the specific material properties of those components which dominated this response. Computer simulations considered various values of elastic modulus, shear modulus, poisson's ratio, density, and thickness of the Ti, GRP, and core. The resulting strain vs. time curves were analyzed, and the conclusions are discussed below. The results described are for a GRP side impact. Ti side impacts displayed similar features, but the tension and compression states were reversed.

a. *Titanium*

Titanium faceplate thickness and elastic modulus were the dominant factors in controlling the maximum tensile strain of the composite beam. Both of these factors appeared to have equal influence. There existed an inverse proportional relationship between each of them and the tensile strain.

b. *Core*

Honeycomb G_{yz} controlled the bending mode shape of the non-impacted surface and the cycle time of the beam's transient deflection. A value of G_{yz} below some threshold allowed the non-impacted surface to enter a second bending mode configuration. (This phenomenon will be discussed in more detail later.) Additionally, if this second mode was experienced, a significant increase in the time required for the beam to return to a zero strain condition was noted.

c. *GRP*

GRP faceplate thickness and E_y were the dominant factors in controlling the maximum compressive strain of the composite beam. Both of these factors appeared to have equal influence. Also, there existed an inverse proportional relationship between each of them and the compressive strain.

Using the results of this parametric study, material properties and thickness dimensions were selected to develop a computer model whose strain vs. time relationship was qualitatively similar to the experimental curves developed by Fuller.

3. Model Validation

Fuller's experimental strain vs. time results for a 0.0254 m (1.0 in) drop height impact on both the GRP and Ti sides are shown in Figures 4 and 5. The results of the

13

finite element analysis using the material properties selected from the parametric study are presented in Figures 6 and 7. Comparing these two sets of figures, it is seen that they are quite similar in geometry and magnitude. In particular, the general shape of the numeric and experimental responses at all measured locations are comparable.

Fringe plots of the γ_{yz} distribution in the core for both GRP and Ti side impacts at the time of maximum vertical displacement are given in Figures 8 and 9. As can be seen, the maximum shear strain is located in the quarter area. This demonstrates where the predicted failure would first occur and is in agreement with the experimental observations.

Quite obviously, this model is not sufficiently accurate for quantitative study of the dynamic response of the sandwich beam subject to low velocity impact because all necessary material properties are not presently available. However, based upon its good correlation with the experimental results in the areas of overall shape of the response curves, maximum peak strain values, and location of maximum shear strain, the model does meet the stated objective of being adequate for a qualitative analysis of the response behavior.
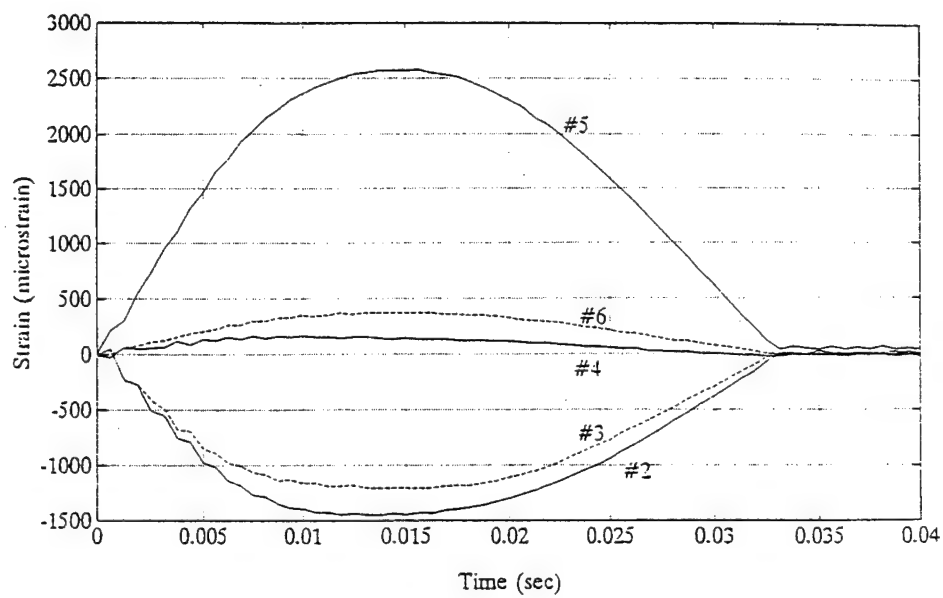
Figure 4. Experimental GRP Normal Strain. From Ref. [1]
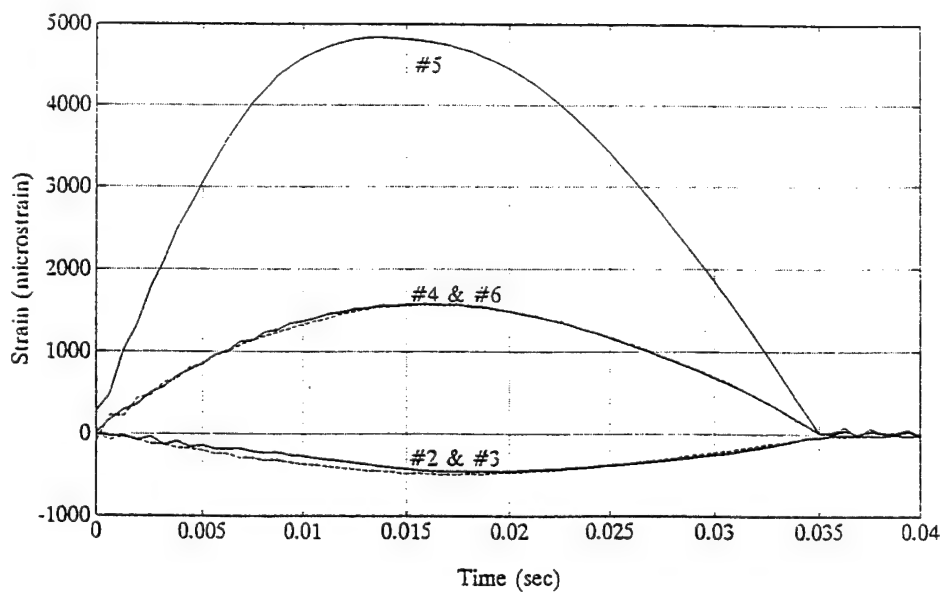

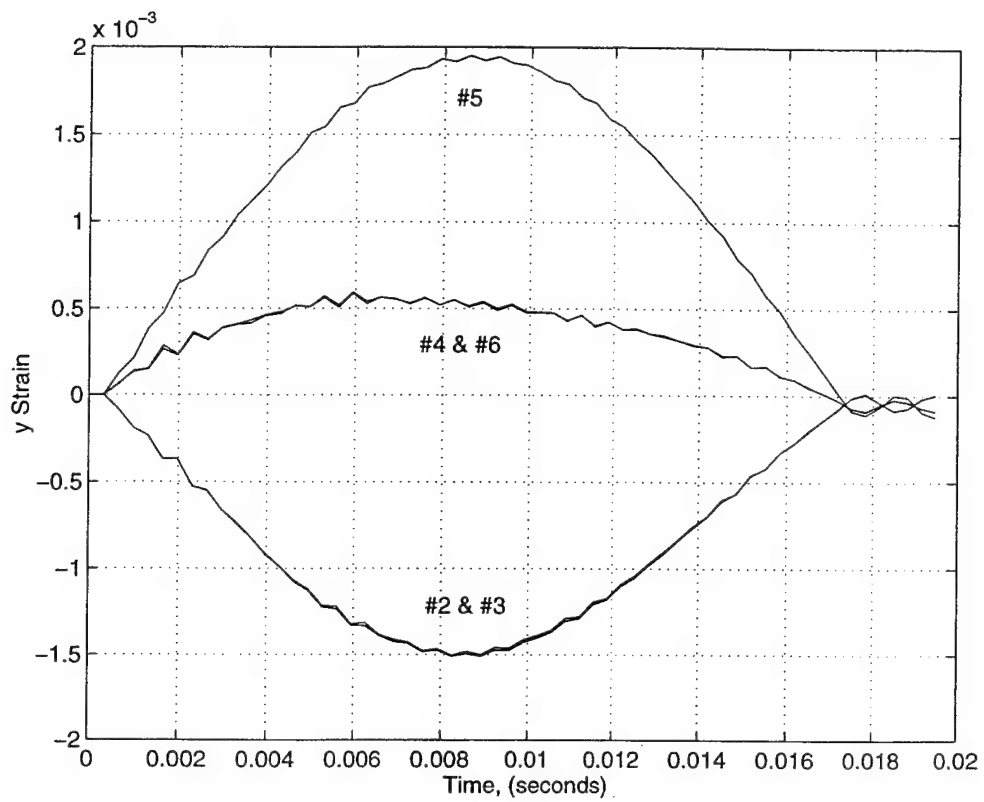Figure 5. Experimental Ti Normal Strain. From Ref. [1]

15

Figure 6. Numerical Normal Strain Response for Impact on GRP Side from
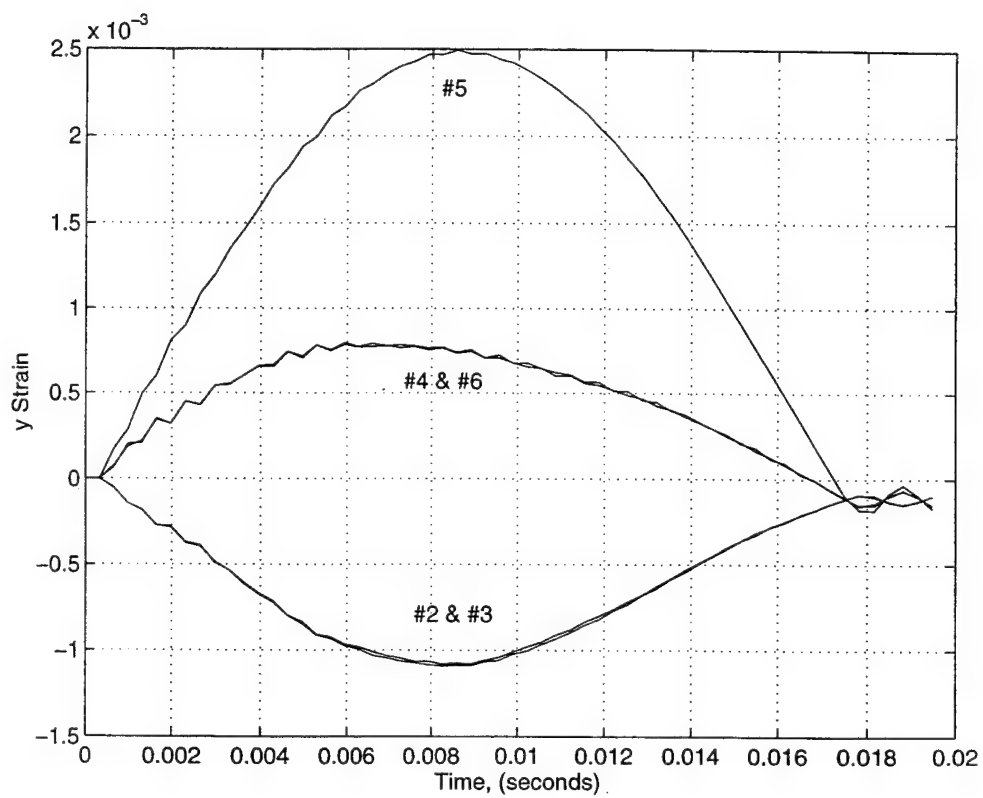0.0254 m (1.0 in)

Figure 7. Numerical Normal Strain Response for Impact on Ti Side from
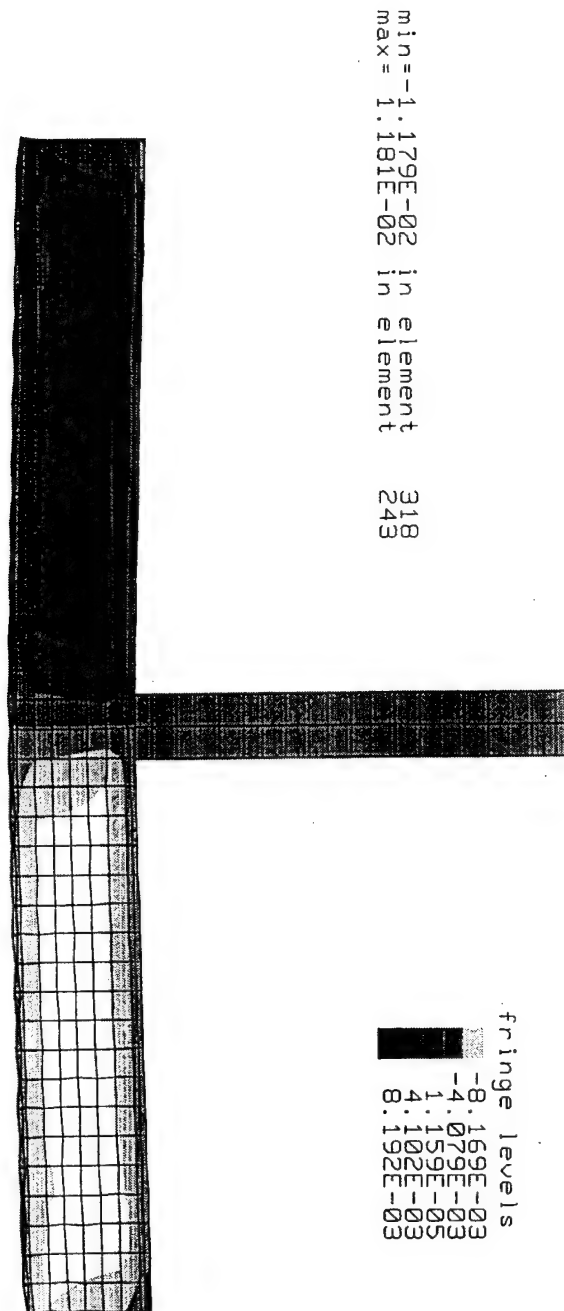0.0254 m (1.0 in)

17

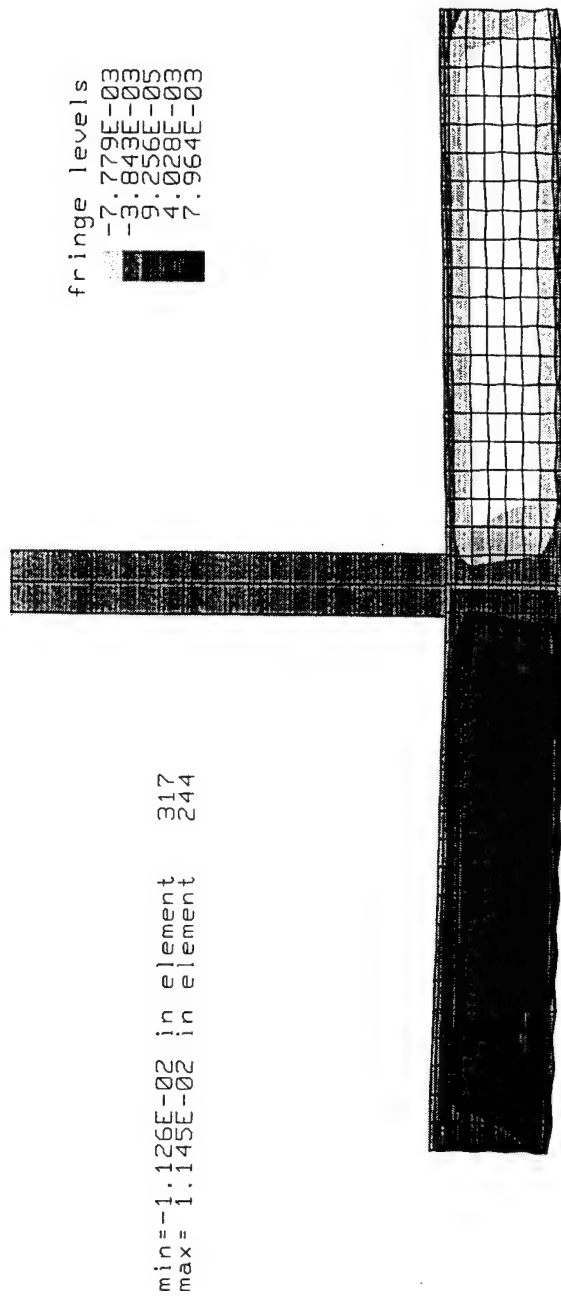Figure 8. Fringes of Maximum γ_{yz} for Impact on GRP Side

Figure 9. Fringes of Maximum γ_{yz} for Impact on Ti Side

19

B.   BALANCED CARBON-FOAM SANDWICH BEAM

The model was a 0.3302 m (13 in), simply supported beam. Again, the model length was based upon the support locations 0.0254 m (1.0 in) from the ends of the actual beam. Core thickness was 0.00635 m (0.25 in) and delamination length was varied. The material properties of Table II were utilized.

The finite element mesh consisted of two elements through thickness for each of the faceplates and four elemenst through thickness for the core. Forty eight longitudinal and two transverse elements were used (See Figure 10).

The impactor was modeled as a rigid, rectangular block with a height of 0.0508 m (2.0 in), a width of 0.01905 m (0.75 in), and a weight of 4.448 N (1.0 lb$_f$). It was positioned 0.000254 m (0.01 in) above the beam, given an initial velocity equivalent to that of a 0.06858 m (2.7 in) free fall, and subjected to gravitational force.

The finite element analysis for the above described model produced a strain vs. time response that was qualitatively representative of the experimental results for both the delaminated and non-delaminated cases. The overall shape of the experimental and FEA curves were quite similar. Based upon this observation, the model was determined to meet the goal of being sufficiently accurate to make qualitative observations as to the sandwich beam's dynamic impact response.

C.   BALANCED CARBON-FOAM SANDWICH PLATE

To take advantage of symmetry and decrease computational time, a quarter-model of a 0.127 m (5.0 in) square, simply supported plate was developed. Component material properties and thickness dimensions were the same as those for the carbon-foam beam.

The finite element mesh consisted of two elements through thickness for each of the faceplates and four elements through thickness for the core. A 0.0254 m (1.0 in) radius polar mesh centered at the plate's center point was utilized to model the impact and delamination areas (See Figure 11).

20

The impactor was modeled as a cylindrical block with a height of 0.0254 m (1.0 in), radius of 0.0127 m (0.5 in), and weight of 8.896 N (2.0 lb$_f$). It was positioned 0.000245 m (0.01 in) above the beam, subjected to gravitational force, and given an initial velocity equivalent to that of a 0.6858 m (27.0 in) free fall.
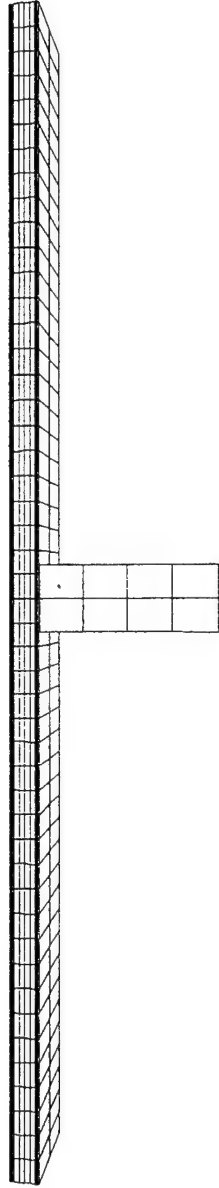
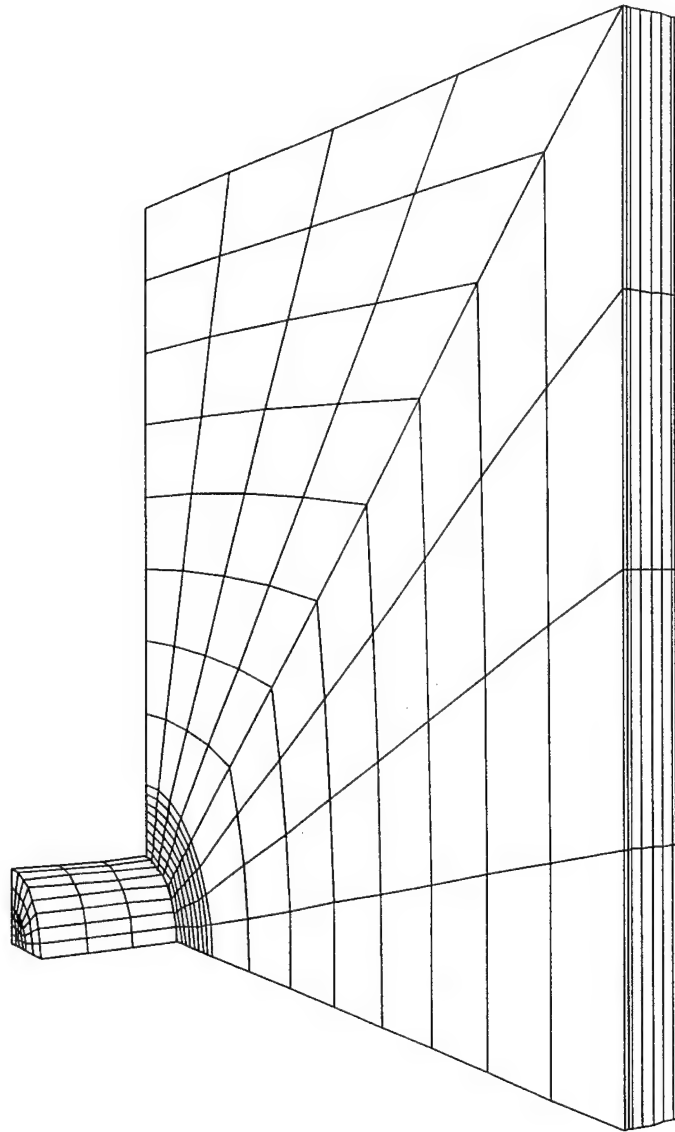Figure 10. FEM Mesh of Balanced Carbon-Foam Sandwich Beam

Figure 11. FEM Mesh of Balanced Carbon-Foam Sandwich Plate

IV. DISCUSSION

A. UNBALANCED TI-HONEYCOMB-GRP SANDWICH BEAM

1. Vertical Displacement

Several observations were made concerning the displacement vs. time response of the unbalanced sandwich. Specifically, these deal with the maximum displacement, the effects of transverse shear and through-thickness deformations, and energy absorbsion of the beam.

First, the magnitude of the maximum displacement of the impacted side of the beam appears to be independent of the side of impact (GRP or Ti). Obviously, the location of this displacement is at the beam's centerline, directly under the impactor. For a beam of uniform construction, equal displacements in response to an impact on either side would be expected, but not necessarily so for an unbalanced composite beam.

Figure 12 shows the model's predicted displacement response for a 0.0254 m (1.0 in) drop height. As can be seen, maximum displacements for the Ti and GRP side impacts are within approximately 8%. Fuller's experimental work gave similar results. He found that maximum displacements were within 15% and that there was no clear trend as to which impact side gave a larger deflection. Therefore, from the numerical and experimental observations, it appears that there is no clear correlation between impacted side and maximum displacement, and that the impacted side and maximum displacement appear to be independent.

Second, the top and bottom faces deform differently, particularly at the point of impact. This is due to the presence of transverse shear and through-thickness deformations in the core. Figure 13 shows the relative deformations of the top and bottom surfaces for a GRP side impact. As can be seen, the centerline radius of curvature of the bottom surface is greater than that of the top surface. Also, the deformations of the two surfaces at the supports are quite different. From these observations, it is apparent that the effect of transverse shear and through-thickness deformations are significant, and they cannot be neglected as in a beam of uniform construction.

Finally, it appears that the transverse shear and through-thickness deformations are not totally elastic. Figure 14 is the experimental velocity vs. time graph of the impactor for a 0.0254 m (1.0 in) drop on the GRP side. As can be seen, it is not a perfect sinusoid. The maximum negative (upward) velocity achieved is significantly less than the impact velocity. The numerical analysis provided a similar result. This characteristic implies that the beam does not act as a perfect spring. Some energy is apparently absorbed in the core deformations. This would follow reasonably from the findings of Nemes and Simmonds [Ref. 3], who reported that a portion of the shear deformations in the core are non or slowly recoverable.
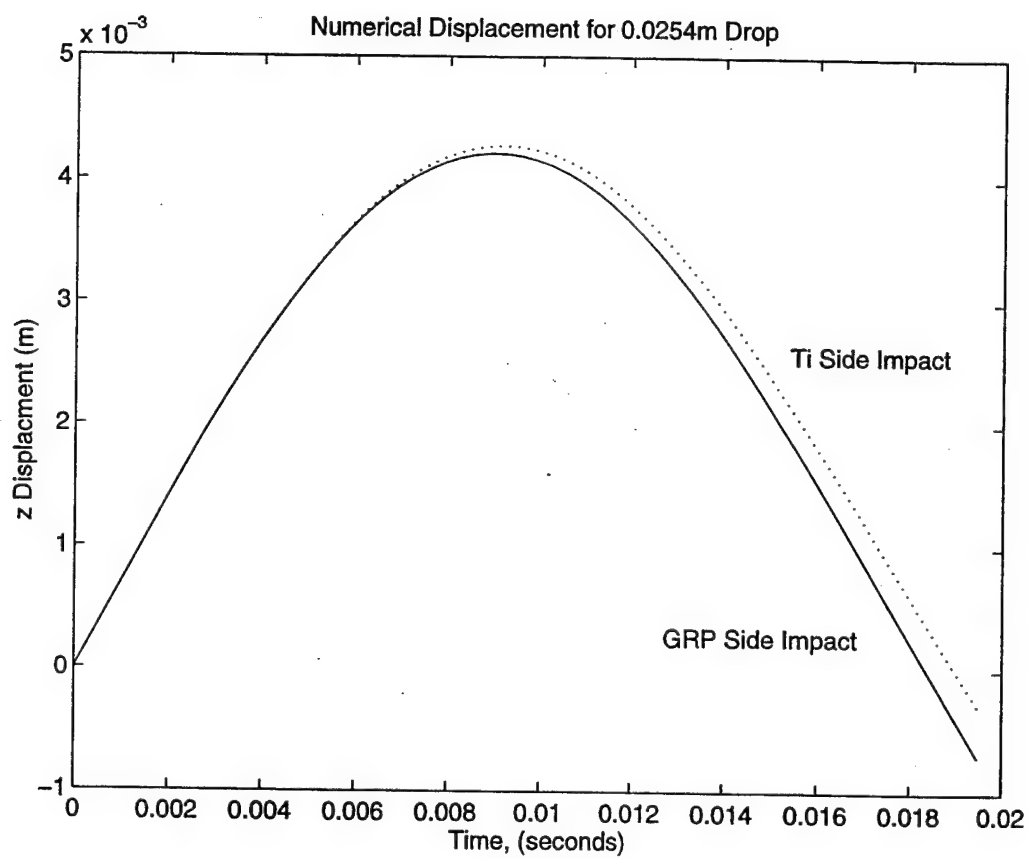
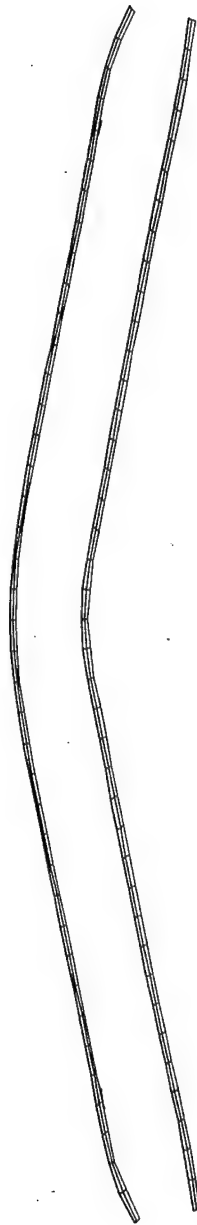Figure 12. Numerical Displacement for 0.0254 m (1.0 in) Drop

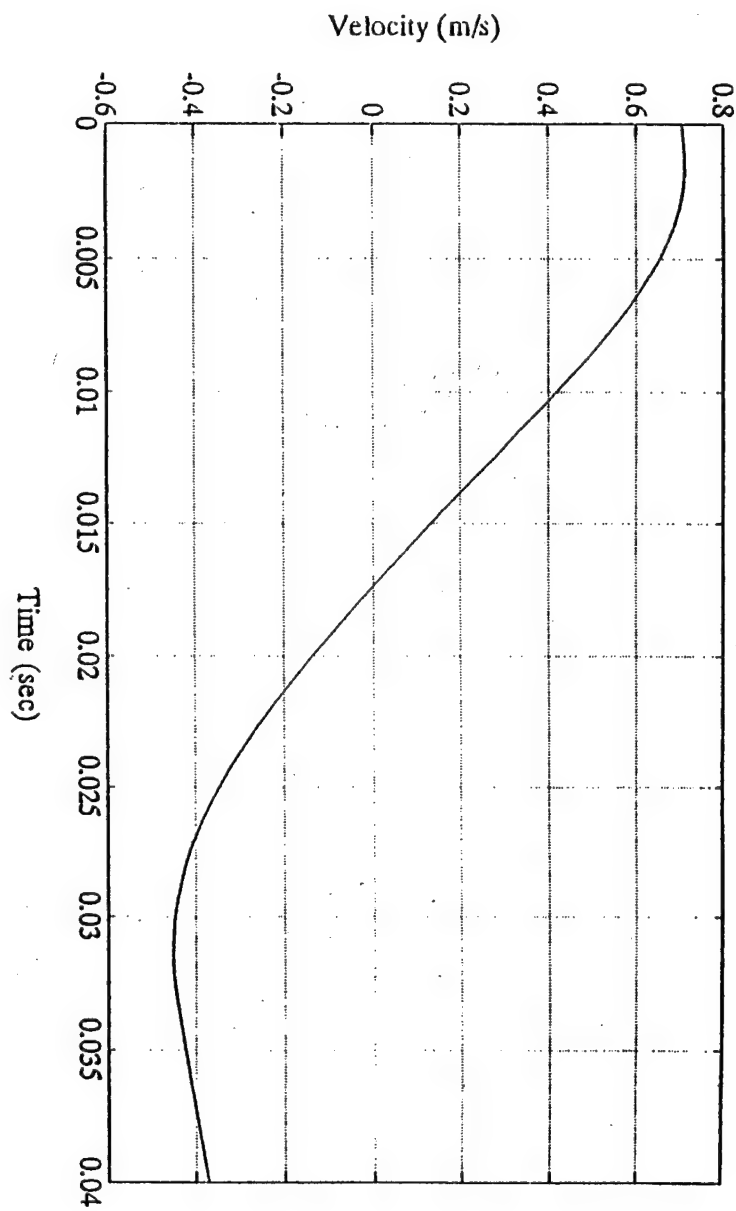Figure 13. Relative Deformations of Impacted and Non-Impacted Surfaces for GRP Side Impact

Figure 14. Experimental Velocity of Impactor for 0.0254 m (1.0 in) Drop on GRP
Side. From Ref [1]

2.   Compressive Strain in the Non-Impacted Surface

In classical beam theory for a three point bending test, it is known that the entire top surface will experience compression while the entire bottom surface is in tension. This is because the beam's neutral axis remains parallel to its horizontal midplane.

The above may not necessarily hold true for a sandwich beam undergoing a dynamic, three point bending test. In particular, the experimental and numerical analysis both indicated that compression may exist in portions of the bottom, non-impacted surface.

Figure 15 shows the classical beam theory and Fuller's experimentally observed deformations of a sandwich beam subject to a three point bending test. As can be seen, the actual observed shape is quite different from what is anticipated from beam theory. Experimental strain gage readings actually showed that portions of the top surface were in tension and that portions of the bottom surface were in compression. A possible explanation for this phenomenon was developed by numerically examining the value of the core material's shear modulus G_{yz} and the response of the sandwich beam's neutral axis.

Figure 16 shows the numerical neutral axis location at maximum displacement for a GRP side impact (dark areas tension, light areas compression). As can be seen, the neutral axis is not parallel to the beam's horizontal centerline. However, the entire bottom surface is in tension. This figure corresponds to the strain-time curve of Figure 6.

Figure 17 also shows the numerical neutral axis location at maximum displacement for a GRP side impact, this time with a G_{yz} value 50% lower than the original model value. In this case, the entire bottom surface is clearly not in tension. Portions are indeed in compression.

Figure 18 gives the strain-time relationships in this state. As can be seen, the bottom surface quarter-point compression manifests itself as a "wave" in the strain-time curve.
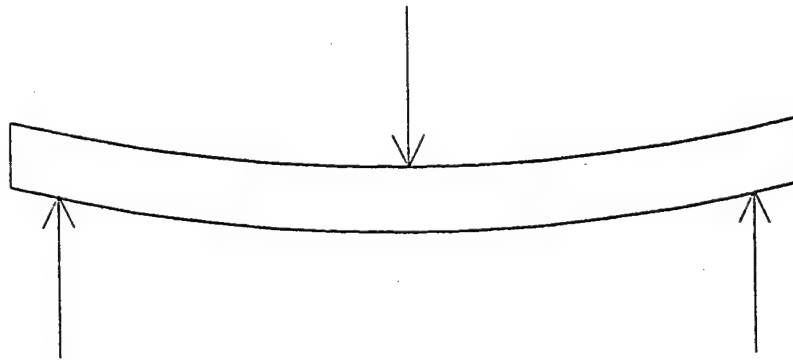
Classical Beam Theory
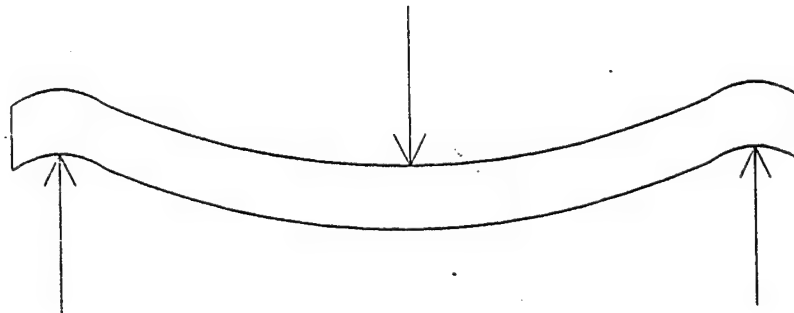
Experimental Findings

Figure 15. Classical Beam Bending Shape vs. Experimental Beam Bending Shape
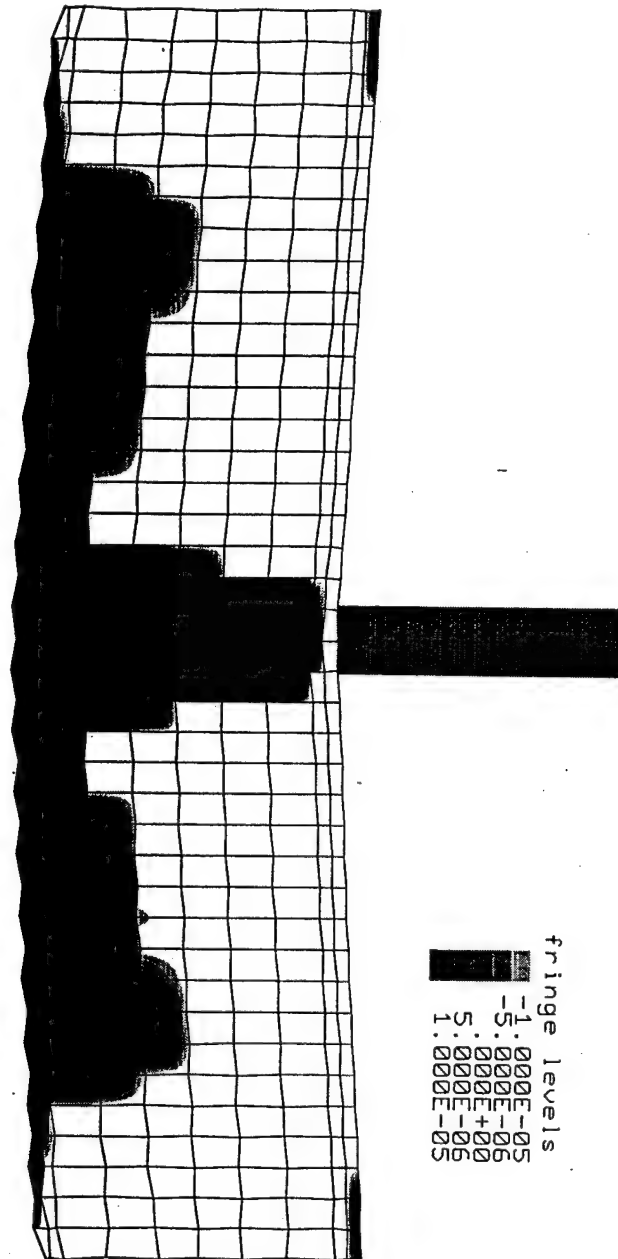From Ref [1]

Figure 16. Neutral Axis Location at Maximum Displacement for GRP Side Impact
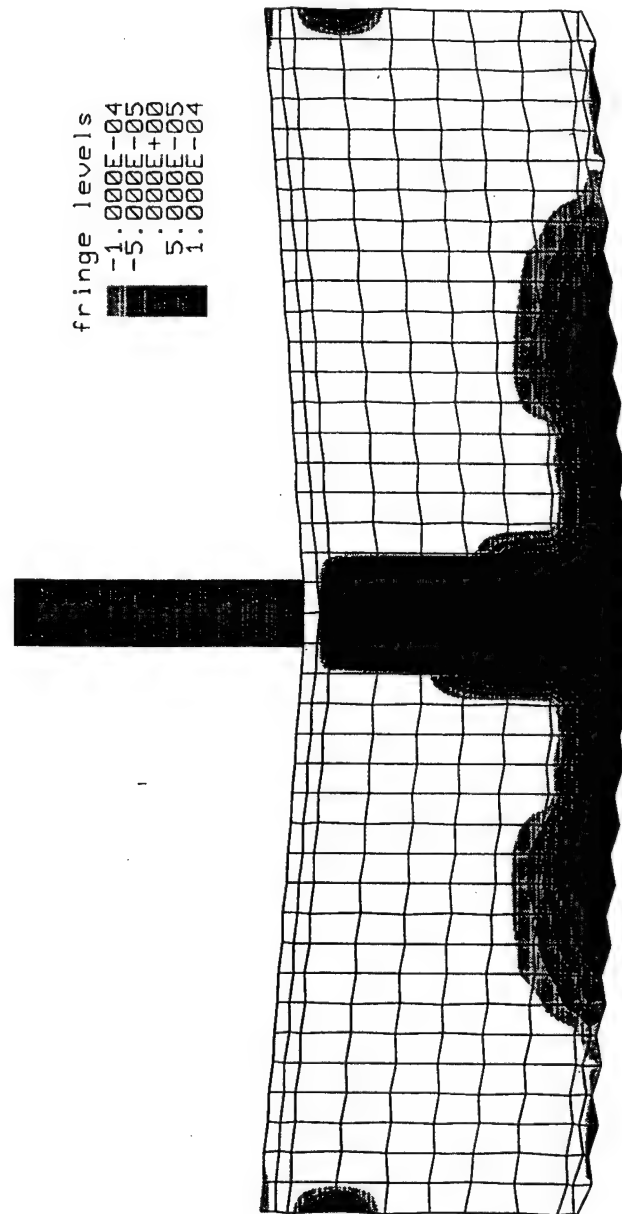
Figure 17. Neutral Axis Location at Maximum Displacement for GRP Side Impact and Reduced Core G_{yz}
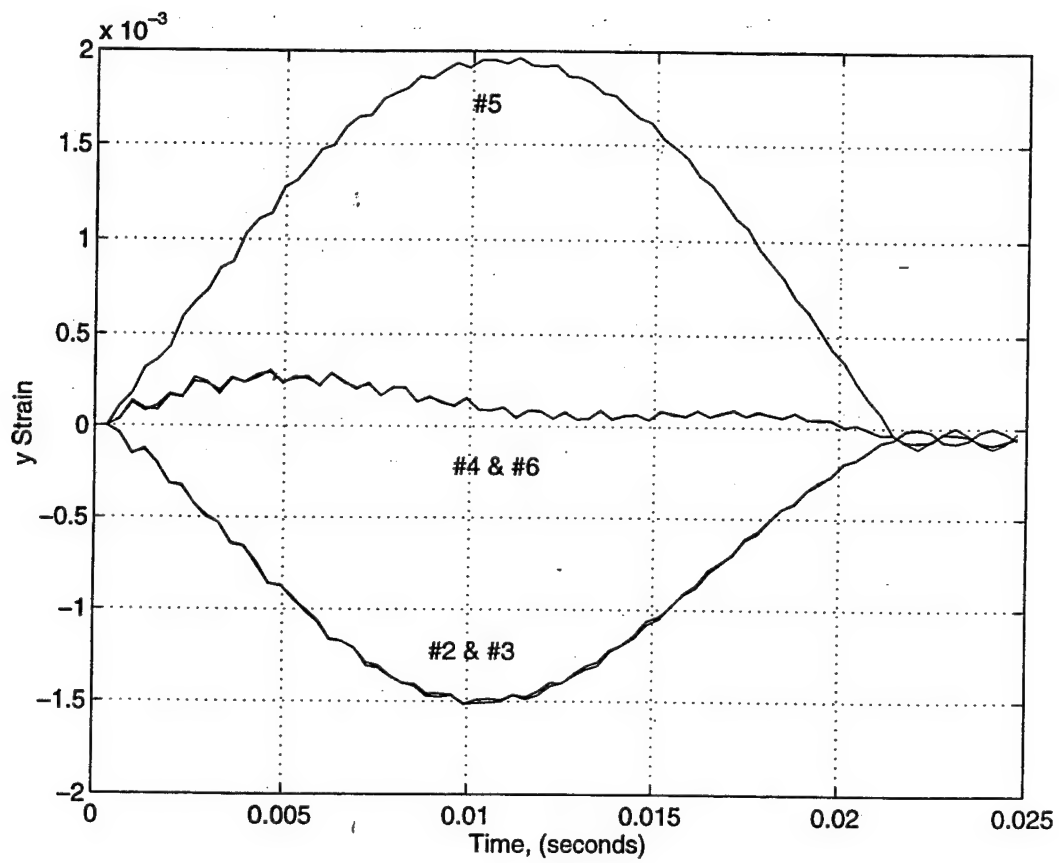
33

Figure 18. Strain Response for Impact on GRP Side and Reduced Core G_{yz}

Figures 19 and 20 show the numerical neutral axis location and the strain-time history for a Ti side impact with the same reduced value of G_{yz}. Obviously, the characteristics are the same as the GRP side impact.

The conclusions to be drawn from these experimental and numerical observations are as follows:

- The neutral axis of a sandwich composite beam undergoing a dynamic, three point bending test may not remain parallel to the beam's horizontal midplane, allowing portions of the bottom, non-impacted surface to enter compression.

- The bottom surface may have a second mode bending configuration.

- There exists a critical value of core shear modulus G_{yz} above which the bottom surface will not enter the second mode bending configuration.

- These phenomenon are impact side independent, occurring in both Ti and GRP side strikes.

The above general conclusions are supported by Fuller's experimental work and the numerical analysis of this study. However, further research is required to confirm the exact nature of these observations.

3.   Failure in Off-Center Impacts

As previously noted, experimental failure of the unbalanced Ti-honeycomb-GRP sandwich beam always occurred in the core due to crimping/shearing. For the case of an impactor strike on the beam centerline, the computer analysis showed that the γ_{yz} distribution in the core was symmetric about the centerline. Referring back to Figure 8, it is seen that the maximum positive and negative values were nearly identical.

Figure 21 is the same fringe plot for a 0.00635 m (0.25 in) offset to right of centerline drop. In this case, the maximum positive and negative shear strains are no longer equal. Additionally, the absolute maximum value, now located on the side of offset, is higher than that of the centerline drop. Similar results were obtained for a Ti side impact.

Again considering the experimental observations, it was noted that core failure was

never symmetric. It failed only on one side, never on both sides. From this observation and the above analysis, it is apparent that one possible cause for such non-symmetric deformation is non-centerline impact.

Taking into account the precision of the drop-weight rig, achieving an exact centerline impact would be very difficult. As a matter of fact, any impact on a beam of this construction may encounter will most likely be off-center. Therefore, the conclusion can be made that, in almost all cases, core shear failure due to impact will be non-symmetric.
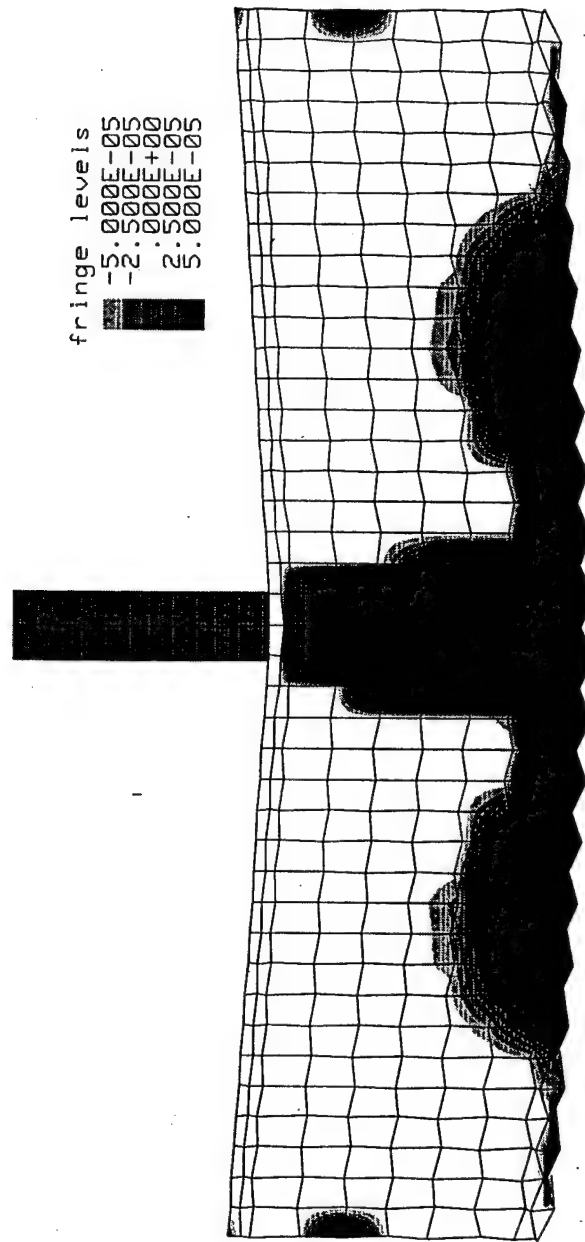
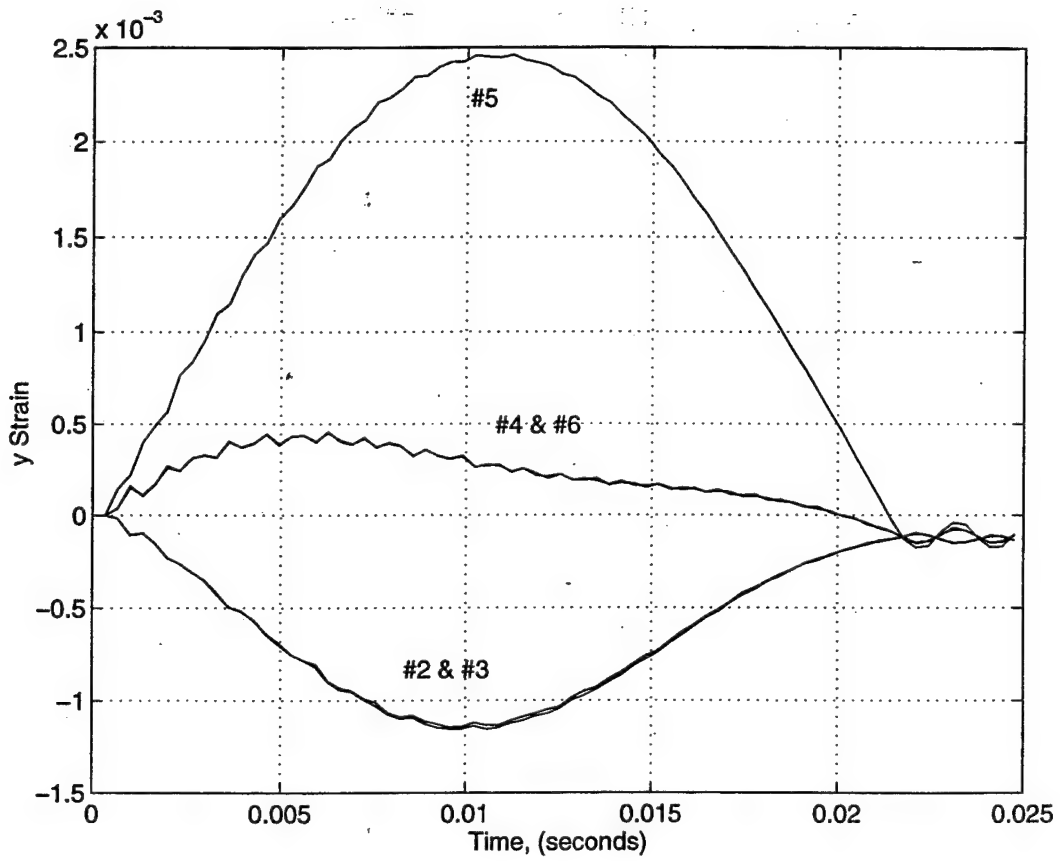Figure 19. Neutral Axis Location at Maximum Displacement for Ti Side Impact and Reduced Core G_{yz}

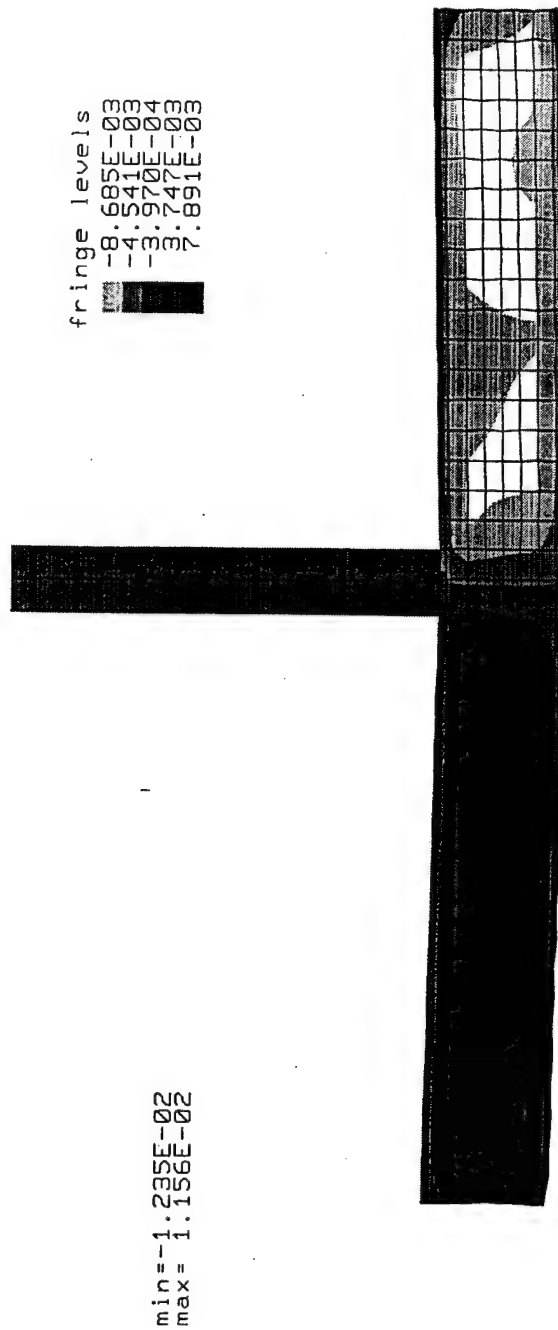Figure 20. Strain Response for Impact on Ti Side and Reduced Core G_{yz}

Figure 21. Fringes of γ_{yz} for a GRP Side Impact and a 0.00635 m (0.25 in) Right of Center Drop Offset

B.   BALANCED CARBON-FOAM SANDWICH BEAM

Clawson experimentally investigated the bending strain vs. time behavior for failure impacts upon the carbon-foam sandwich beam in the cases of no delamination, 0.0127 m (0.5 in) delamination, and 0.0254 m (1.0 in) delamination, respectively. Delaminations were located between the core and the faceplate on the non-impacted side, were centered on the beam centerline, and extended through the entire width of the beam. Significant findings of his investigation were:

- In the case of no delamination and 0.0254 m (1.0 in) delamination, failure occurred in the core in the quarter area and was due to shearing.

- In the case of 0.0127 m (0.5 in) delamination, failure occurred in the bottom faceplate at the centerline and was due to bending.

- The drop height to cause failure (failure load) was higher in the case of a 0.0127 m (0.5 in) delamination than it was in the case of no delamination. Failure load for a 0.0254 m (1.0 in) delamination was less than that for no delamination.

To attempt to explain these observations, computer model simulations were run for 0.0127 m (0.5 in), 0.0254 m (1.0 in), and 0.0381 m (1.5 in) delaminations, as well as the non-delaminated case. The resulting bending strain vs. time graphs are shown in Figures 22-25. Additionally, the resulting shear strain vs. time grahps for the core element recording the highest γ_{yz} in each case are presented in Figures 26-29. Significant data from these figures is presented in Table III.
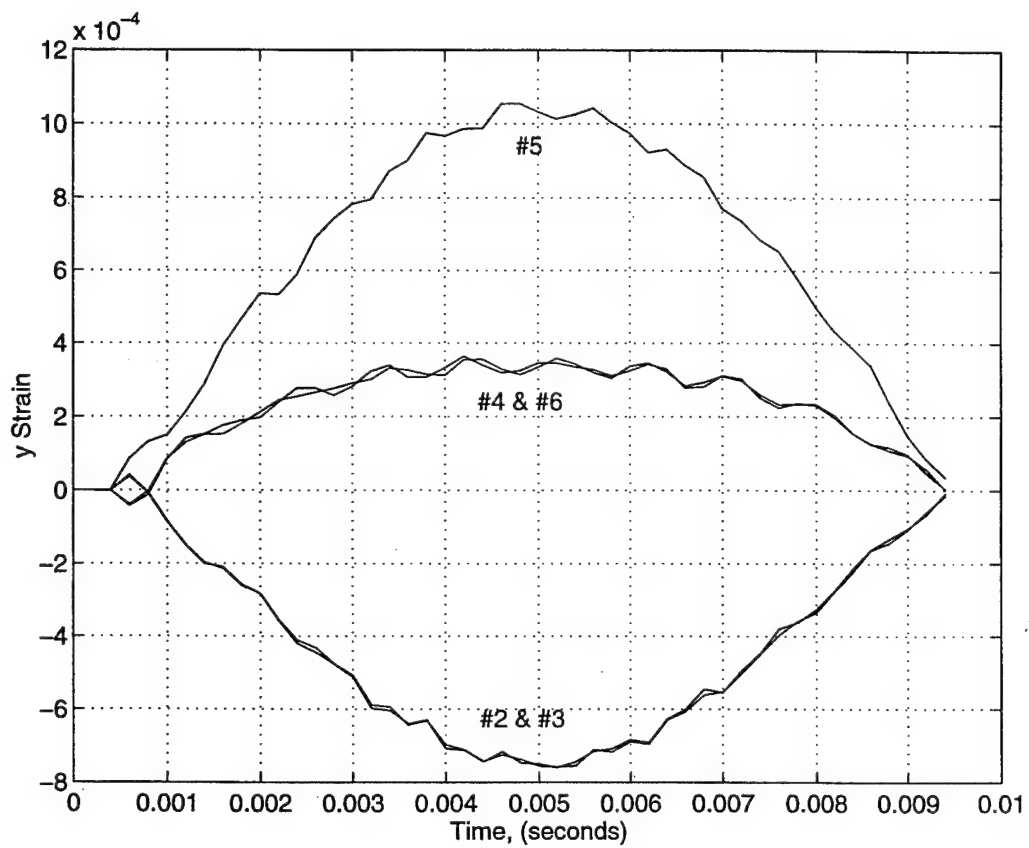
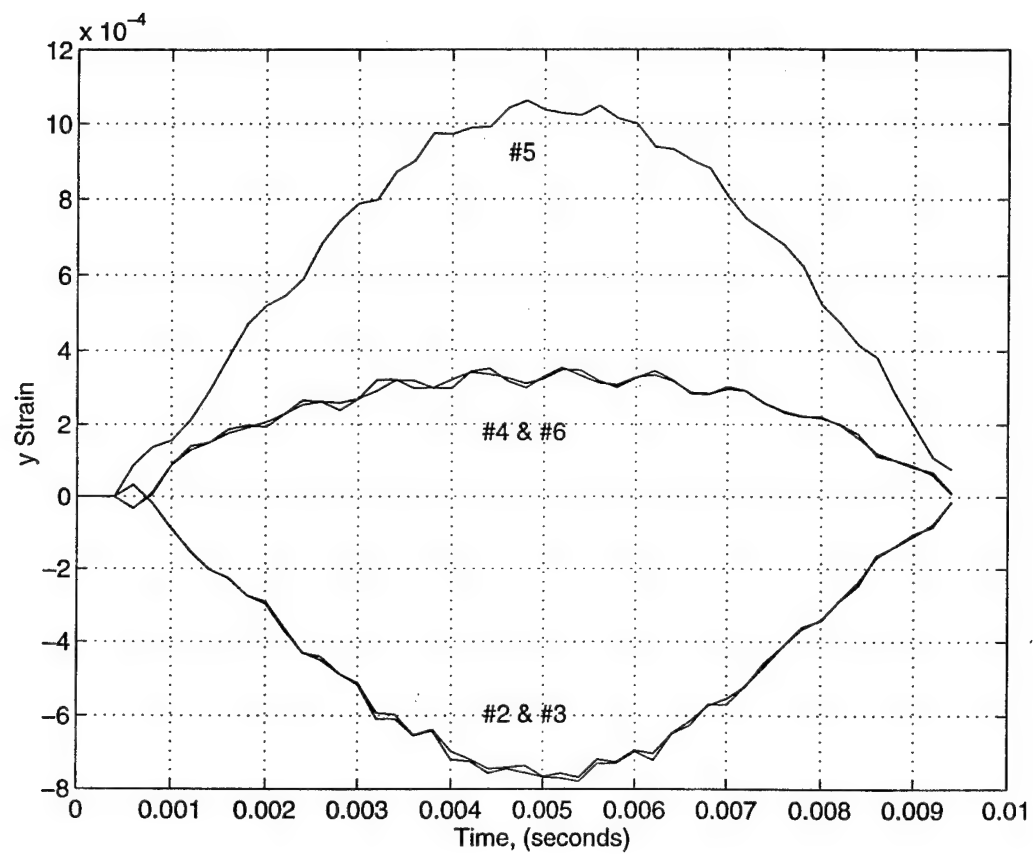Figure 22. Strain Response for No Delamination

Figure 23. Strain Response for 0.0127 m (0.5 in) Delamination

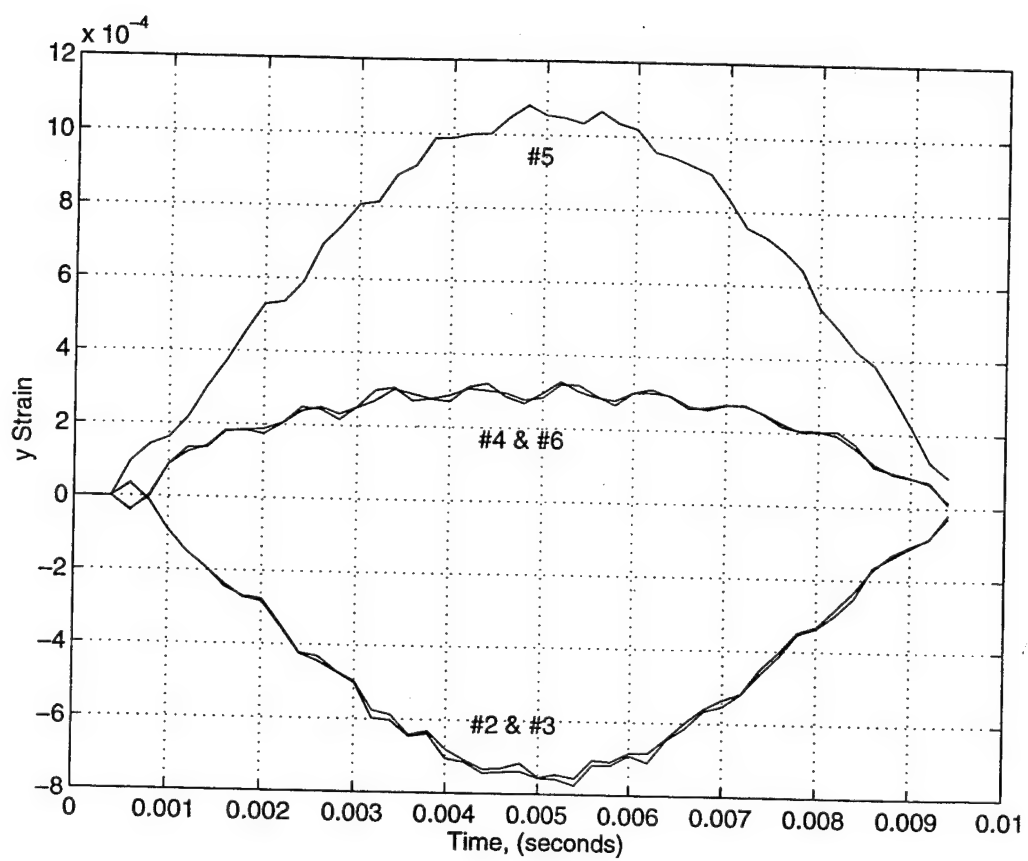Figure 24. Strain Response for 0.0254 m (1.0 in) Delamination
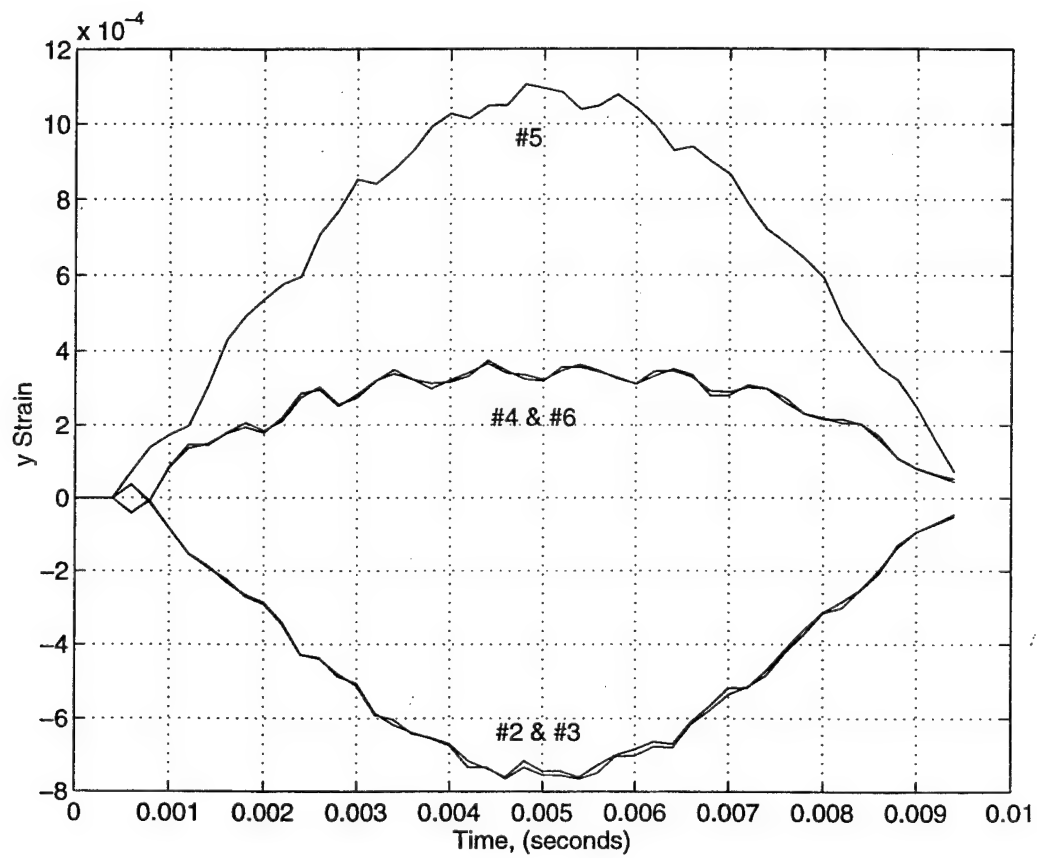
43

Figure 25. Strain Response for 0.0381 m (1.5 in) Delamination
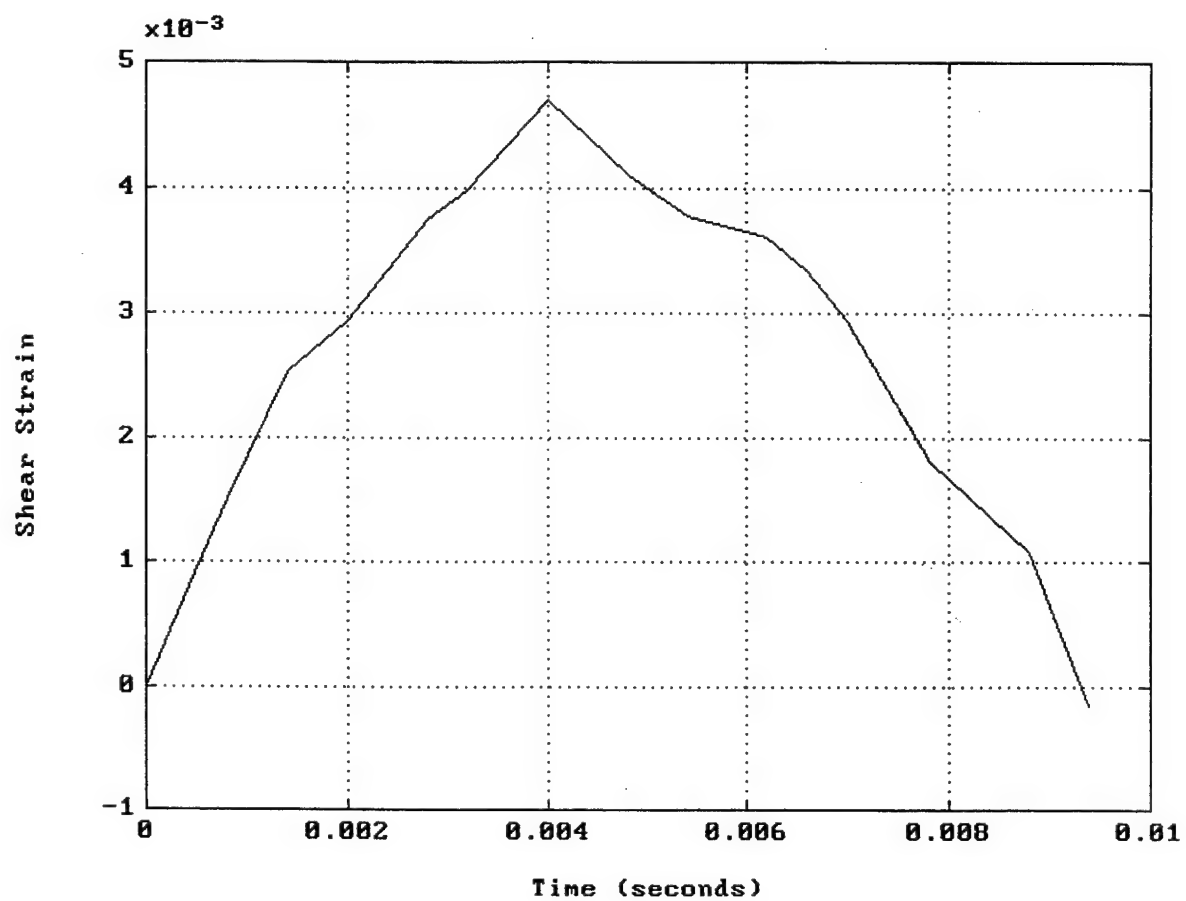
Figure 26. Maximum Core Shear Strain for No Delamination
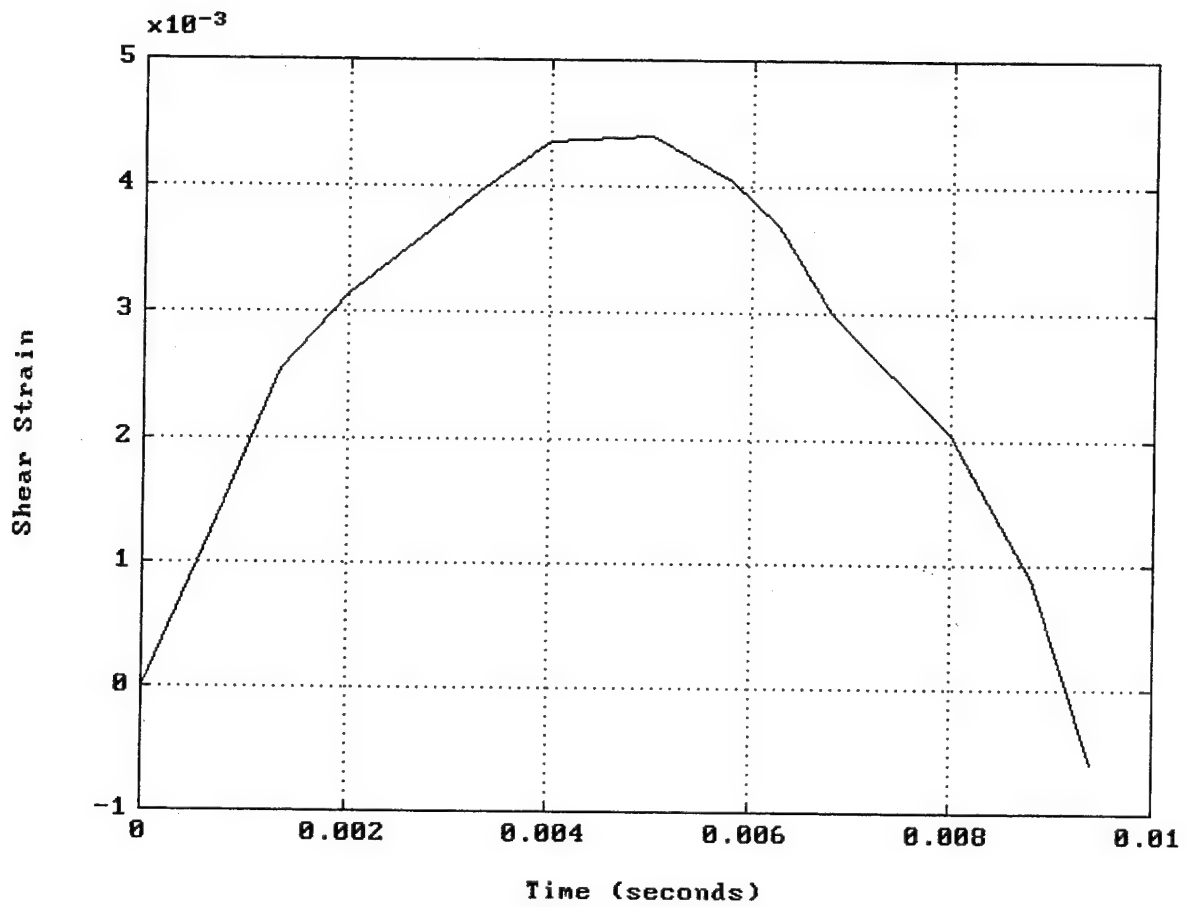
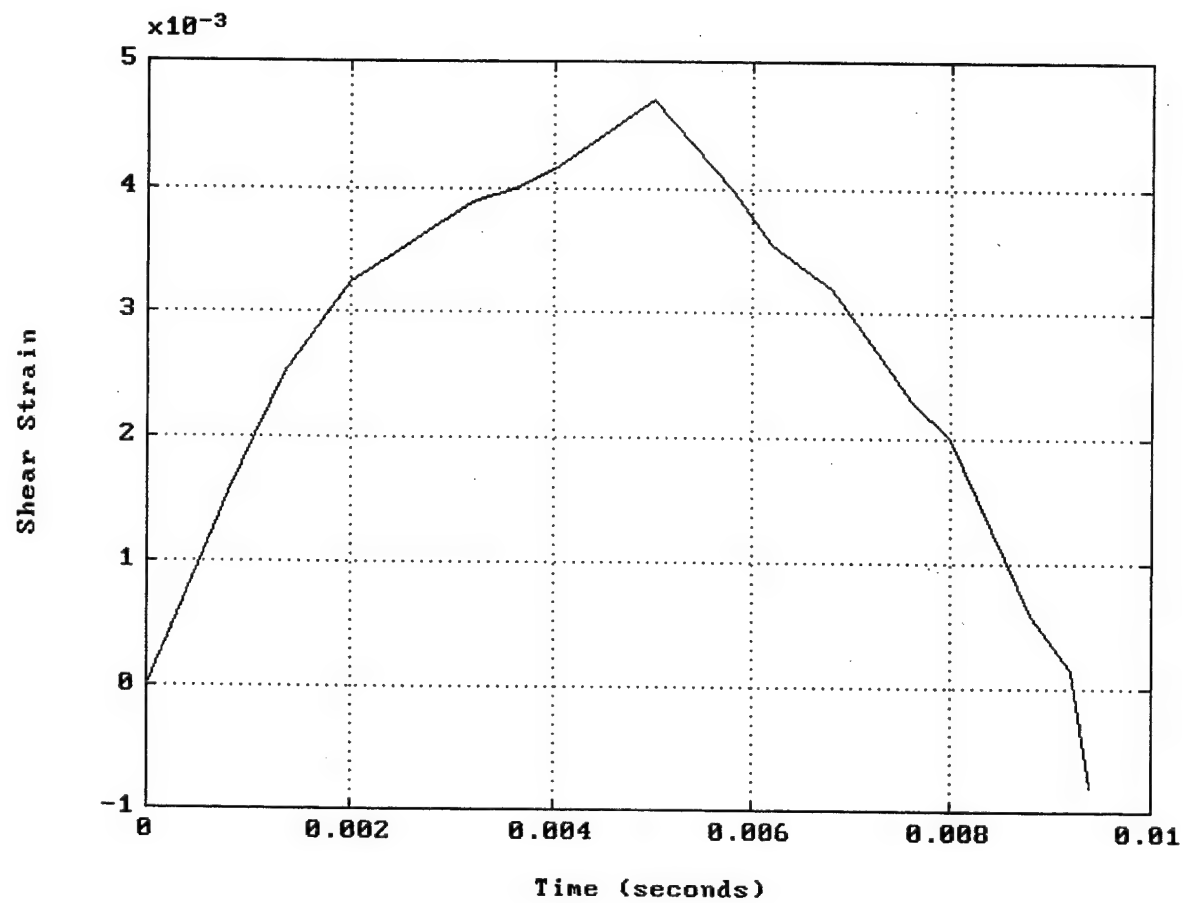Figure 27. Maximum Core Shear Strain for 0.0127 m (0.5 in) Delamination

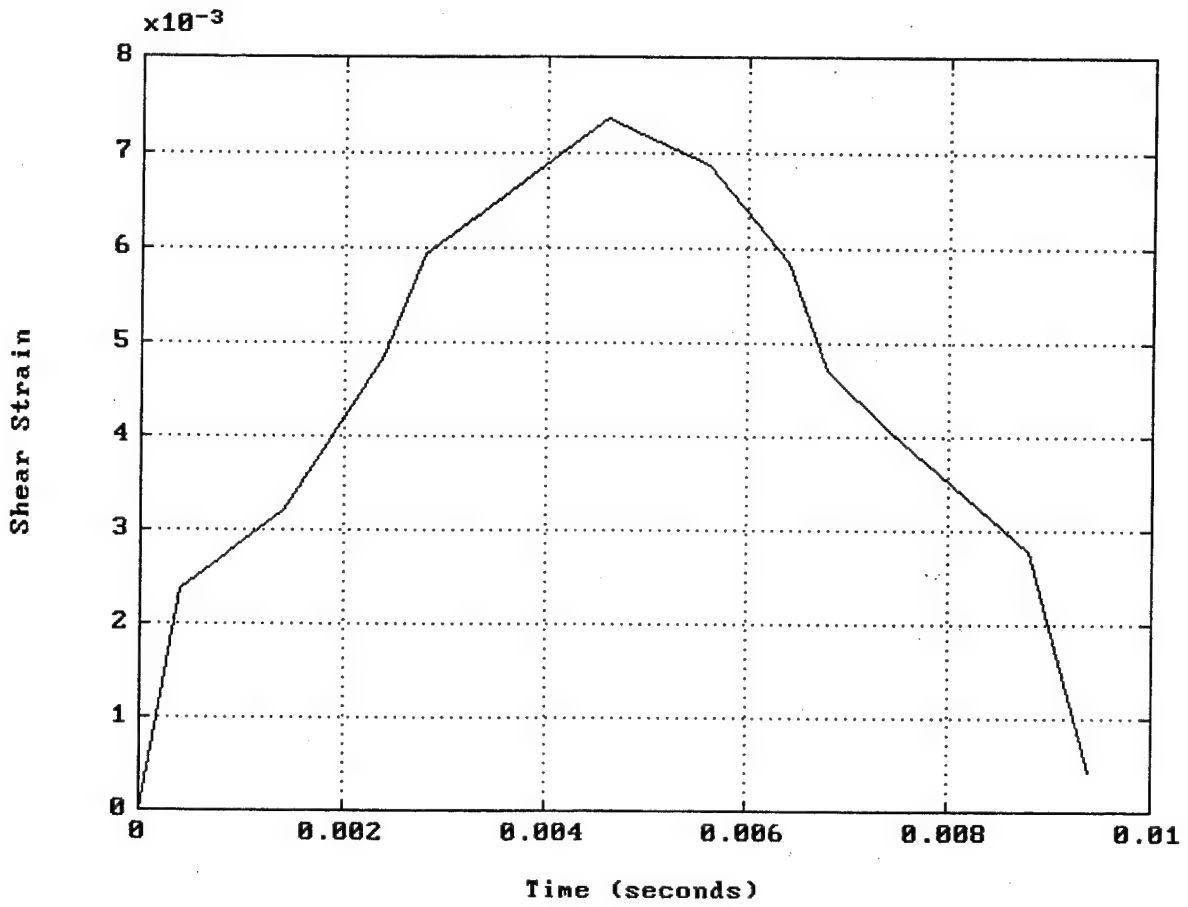Figure 28. Maximum Core Shear Strain for 0.0254 m (1.0 in) Delamination

Figure 29. Maximum Core Shear Strain for 0.0381 m (1.5 in) Delamination

Table III. Carbon Foam Beam Numerical Strain Results

Delam Size (m)(in)	ε_y max (x10^{-3})	ε_y Δ*	γ_{yz} max (x10^{-3})	γ_{yz} Δ*	γ_{yz} max Location
None	1.119	-	4.697	-	Qtr Area**
0.0127 (0.5)	1.094	-2.2%	4.342	-7.6%	Qtr Area
0.0254 (1.0)	1.115	+0.3%	4.645	-1.1%	Qtr Area
0.0381 (1.5)	1.160	+3.7%	7.366	+56.8%	Delam Tip

* Percent change from non-delaminated value
** Qtr Area defined as general length between the beam support and center line

Analyzing the data in Table III, the failure location and failure load of the experimental results can be explained.

In the experimental non-delaminated case, failure occurred in the core in the quarter area and was due to shearing, as previously mentioned. This implies that maximum bending strength σ_y (ε_y) in the lower faceplate was not exceeded and that τ_{yz} (γ_{yz}) in the core was the limiting factor.

Using the numerical analysis for a basis of comparison, it can be seen that, in the case of a 0.0127 m (0.5 in) delamination, both the maximum ε_y and maximum γ_{yz} decreased relative to the no delamination case. However, the drop in γ_{yz} was 3.5 times greater than that in ε_y. This implies two things. First, the allowable applied load prior to failure increased. Second, assuming that the beam was near its bending strength limit to begin with, a larger applied load would lead to failure due to faceplate bending at the centerline rather than core shear. Recalling the experimental results, this is exactly what was observed.

Now observing the data for a 0.0254 m (1.0 in) delamination, it is noted that the maximum ε_y and maximum γ_{yz} both increased back to nearly the values of the non-delaminated case. At this point, shear stress was again the liming factor, and experimental failure occurred in the quarter area of the core.

Further increasing the delamination size to 0.0381 m (1.5 in) led to a large jump in maximum γ_{yz}. It also led to a change in location within the core where this shear strain occurred. Rather than in the quarter area, maximum γ_{yz} was located at the edge of the delamination.

The delamination between the faceplate and the core is actually a crack in the beam. As with all cracks, the delamination acts as a stress concentrator. For a Mode I (tensile) crack, the relationship between crack length and the stress intensity factor at the crack tip, K_I, is given by:

$$K_I \propto \sigma_o(a)^{0.5}$$

where σ_o is the magnitude of the nominal applied tensile stress and a is the length of the crack surface. Clearly, as the the crack length increases, there is a corresponding rise in the stress intensity factor.

In a three point bending test, the delamination is actually subject to Mode II cracking (sliding) (See Figure 30). An equivalent relationship to the above exists between the crack length and the stress intensity factor of the second mode. Accordingly, as the size of crack increases, so does the shear stress intensity factor.

Therefore, it is seen that, in the case of no delamination or a small delamination, maximum shear stress in the core occurs in the quarter area. However, as the delamination grows, the stress intensity factor increases, and the location of the maximum shear stress shifts to the delamination tip, causing failure in this position. Figures 31-34 show fringe plots of maximum core shear strains for all cases. Figure 35 gives a fringe plot of the bottom of the core (0.0381 m/ 1.5 in. delamination), displaying the maximum strain location at the delamination tip.
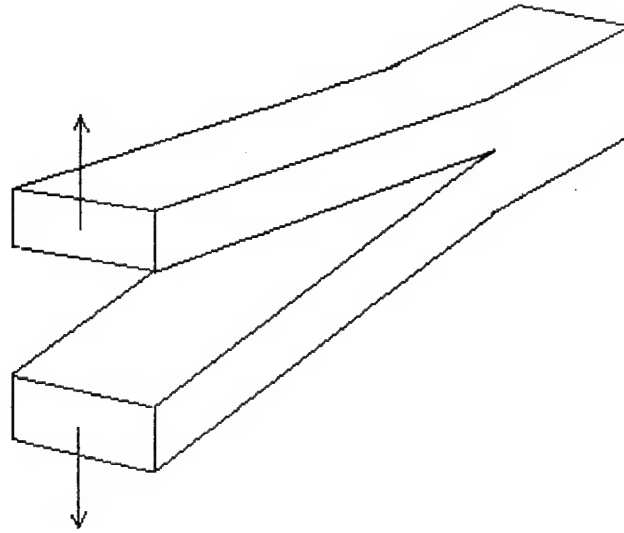
Mode I (tensile)
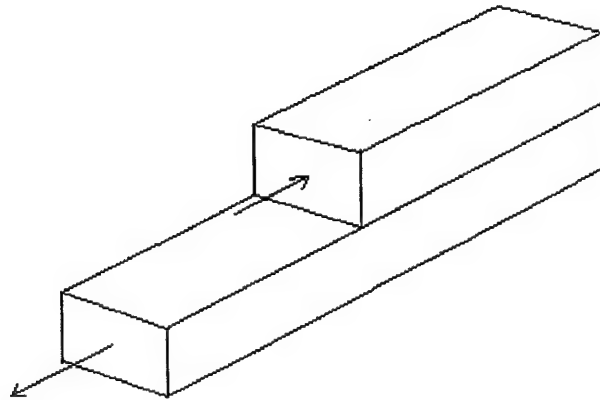
Mode II (sliding)

Figure 30. Cracking Modes
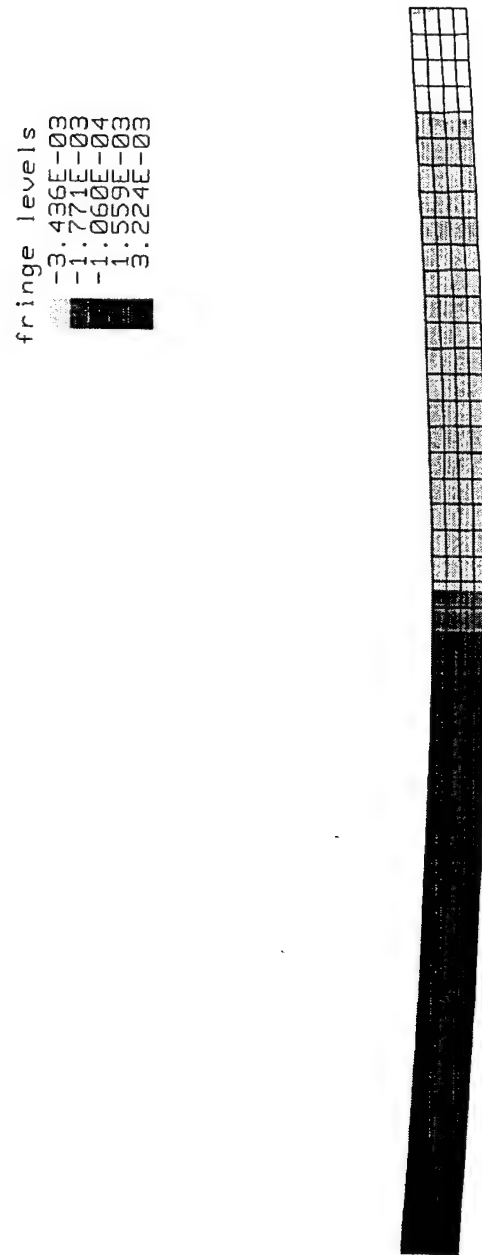
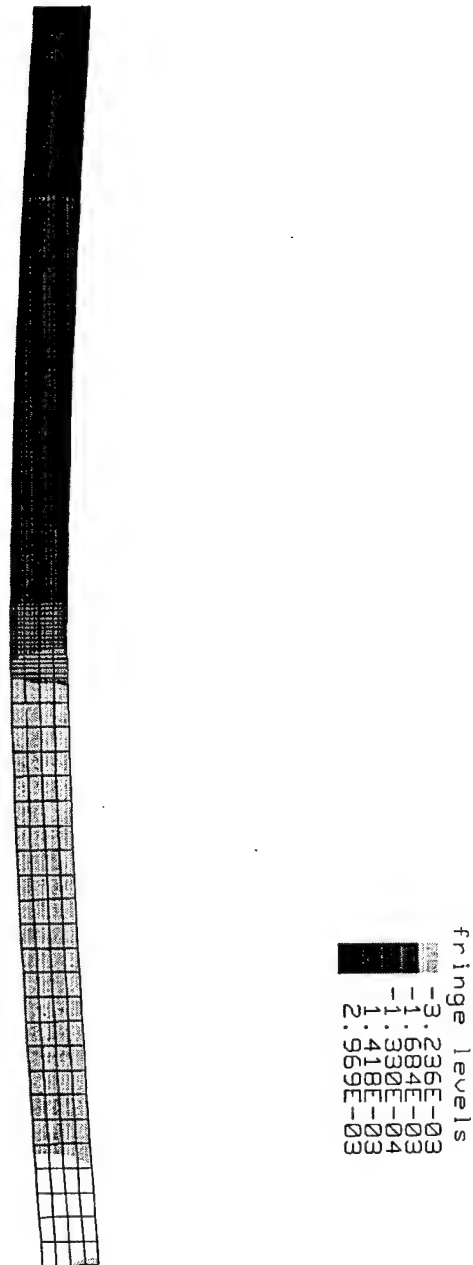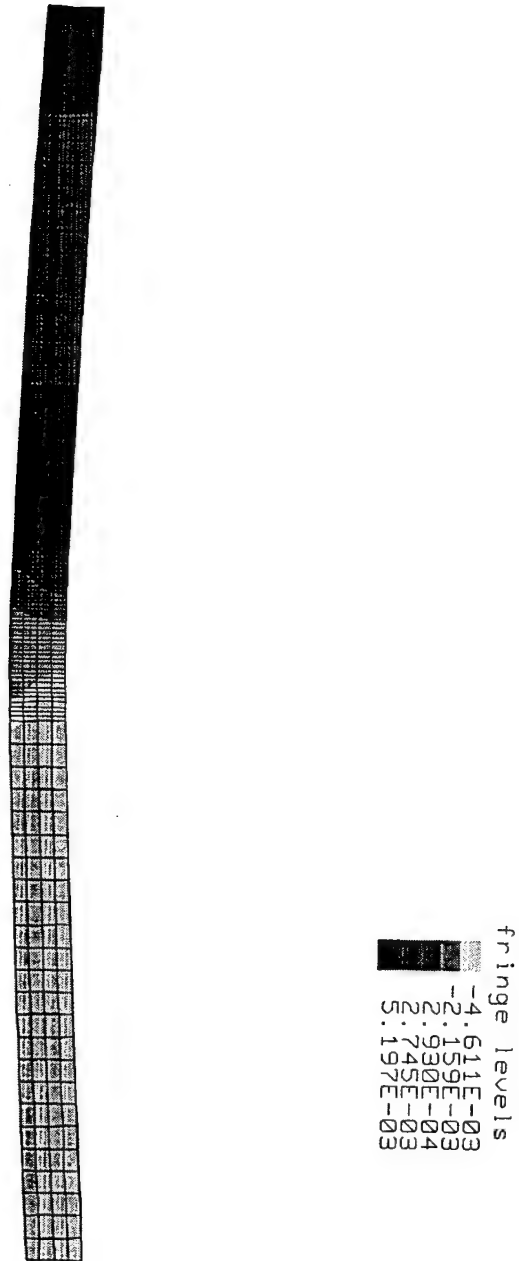Figure 31. Fringes of Core γ_{yz} for No Delamination

Figure 32. Fringes of Core γ_{yz} for 0.0127 m (0.5 in) Delamination

Figure 33. Fringes of Core γ_{yz} for 0.0254 m (1.0 in) Delamination

Figure 34. Fringes of Core γ_{yz} for 0.0381 m (1.5 in) Delamination
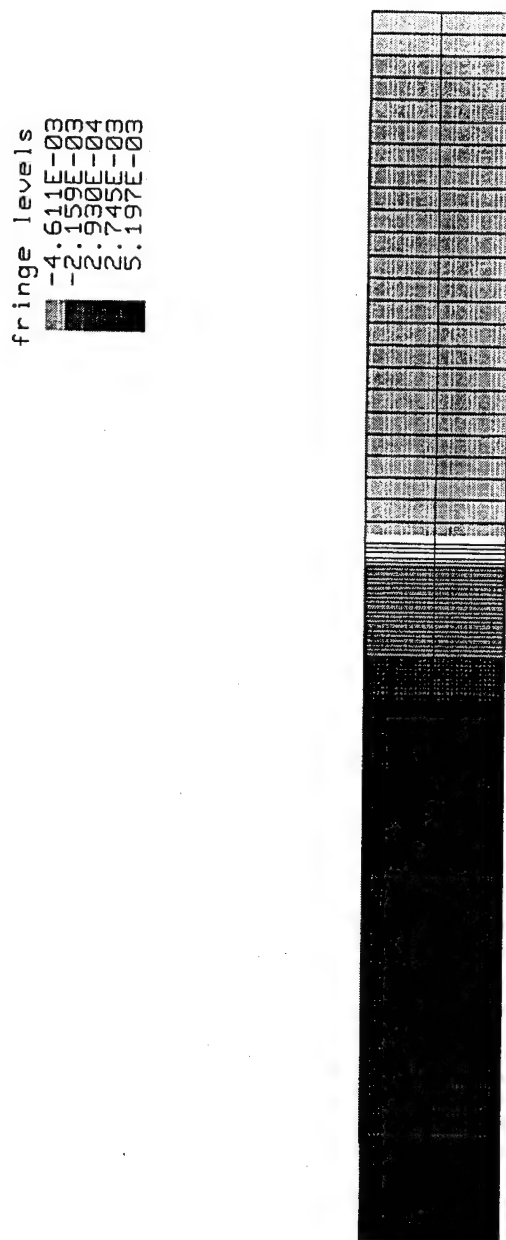
Figure 35. Fringes of Core γ_{yz} for 0.0381 m (1.5 in) Delamination (Bottom View)

C.   BALANCED CARBON-FOAM SANDWICH PLATE

In structural components utilizing sandwich construction, the plate is more often utilized than the beam. However, limited experimental work has been done in this area. To examine a sandwich plates's response to low velocity impact, particularly with respect to an existing delamination, the computer model of the carbon-foam beam was extended to a plate. With this model, four specific areas were examined: vertical deflection, maximum shear stress, delamination detection, and the effect of friction in the delamination area.

In the case of no delamination, fringes plots of the development of the displacement vs. time characteristics are given in Figures 36-42. As can be seen, the fringes of displacement radiate outward from the center after impact. (Slight asymmetry is due to numerical error in the computer modelling.)   This response is normal and expected. Figure 43 gives the displacement vs. time response of the position which experiences the greatest deflection, the midpoint.

Figures 44-50 show the development of the maximum shear stress in the core over time after impact. Again, as expected, the fringe radiates outward from the center. (Variation in outermost fringe due to changing fringe levels. Asymmetry still present.) Figures 51-53 show that the location of maximum shear occurs at the bottom of the core, just outside the radial dimension of the impactor (radial area, for lack of a better name). The maximum shear stress vs. time characteristic of this point is given in Figure 54.

The deflection and shear stress characteristics of a plate with delaminations of 0.01016 m (0.4 in), 0.0127 m (0.5 in), and 0.0254 m (1.0 in) radii were then examined. In general, the development of these characteristics through the plate were identical to that of the non-delaminated case. The maximum values of deflection and core shear stress are given in Table IV.
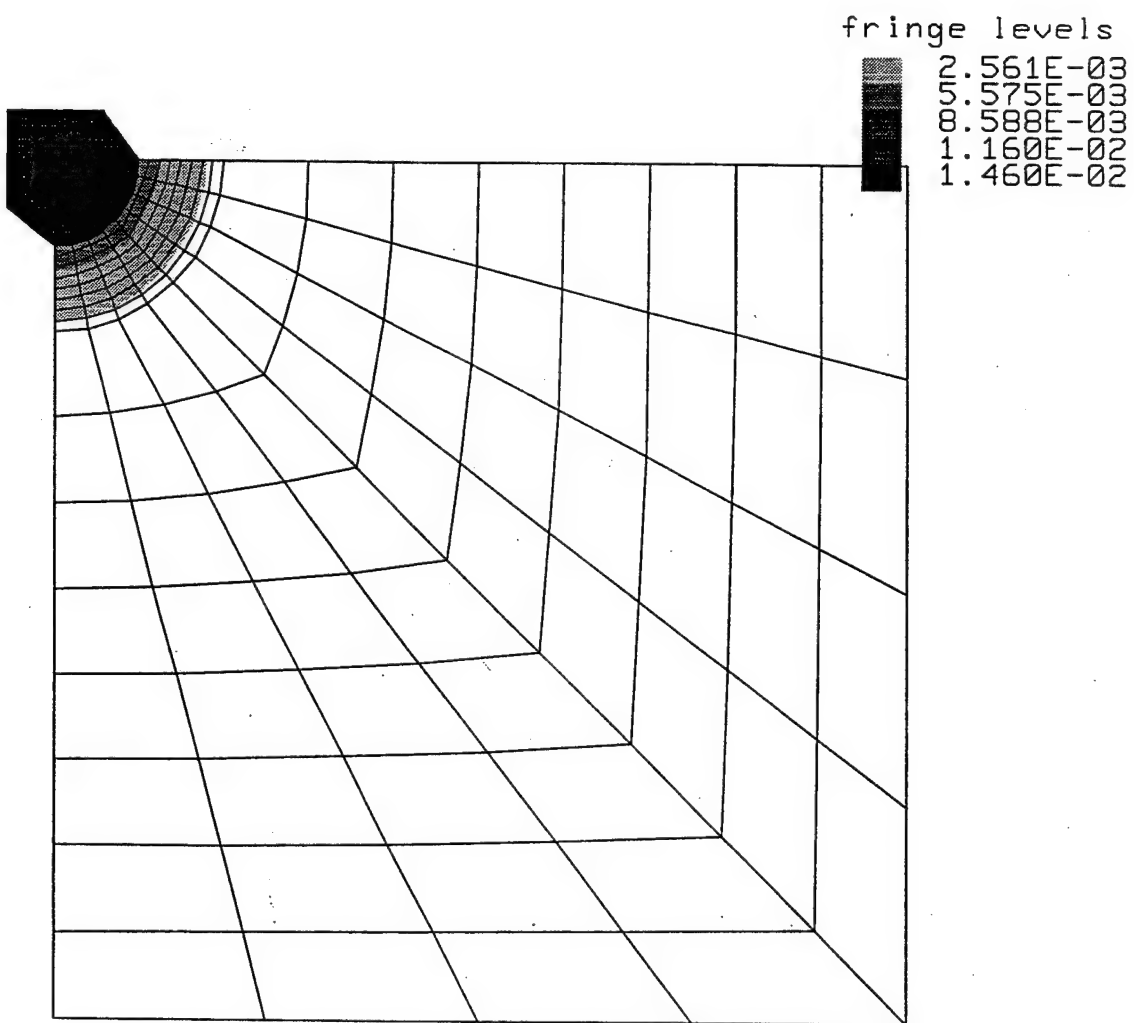
Figure 36. Fringes of z Displacement in Inches (Top View of Plate, t=0.11995x10^{-3} s)

Figure 37. Fringes of z Displacement in Inches (Top View of Plate, t=0.23999x10^{-3} s)

Figure 38. Fringes of z Displacement in Inches (Top View of Plate, t=0.35996x10^{-3}s)
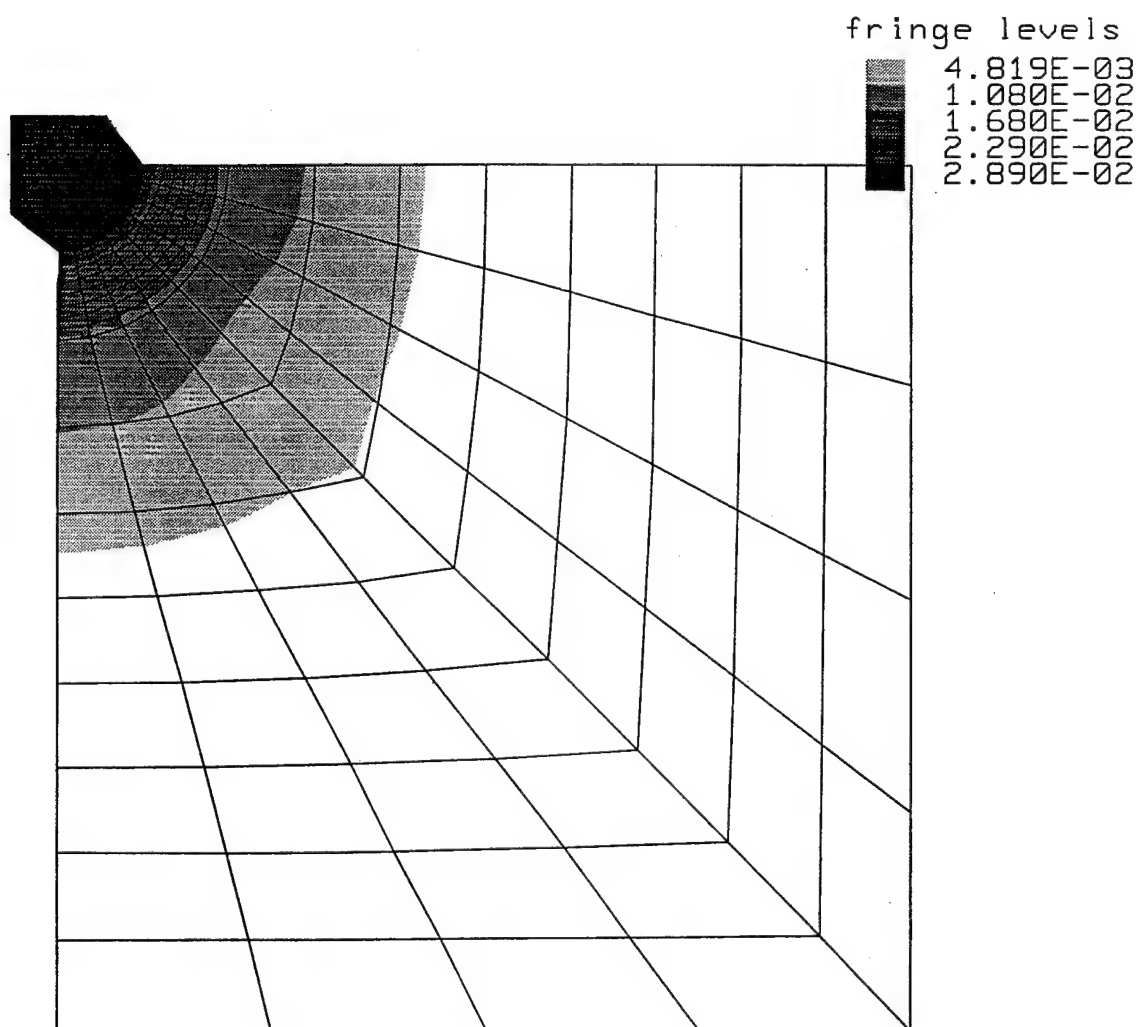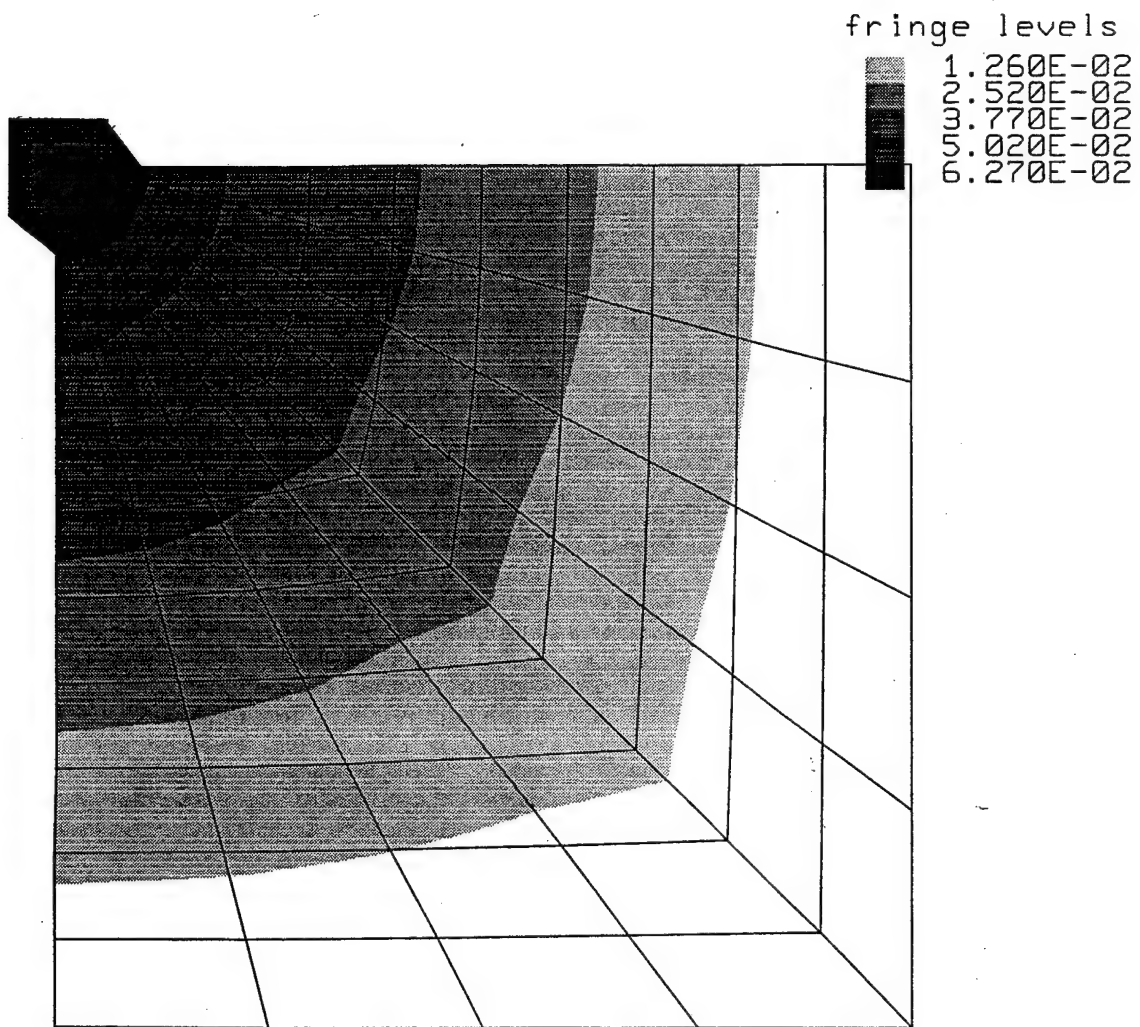
Figure 39. Fringes of z Displacement in Inches (Top View of Plate, t=0.53998x10^{-3} s)
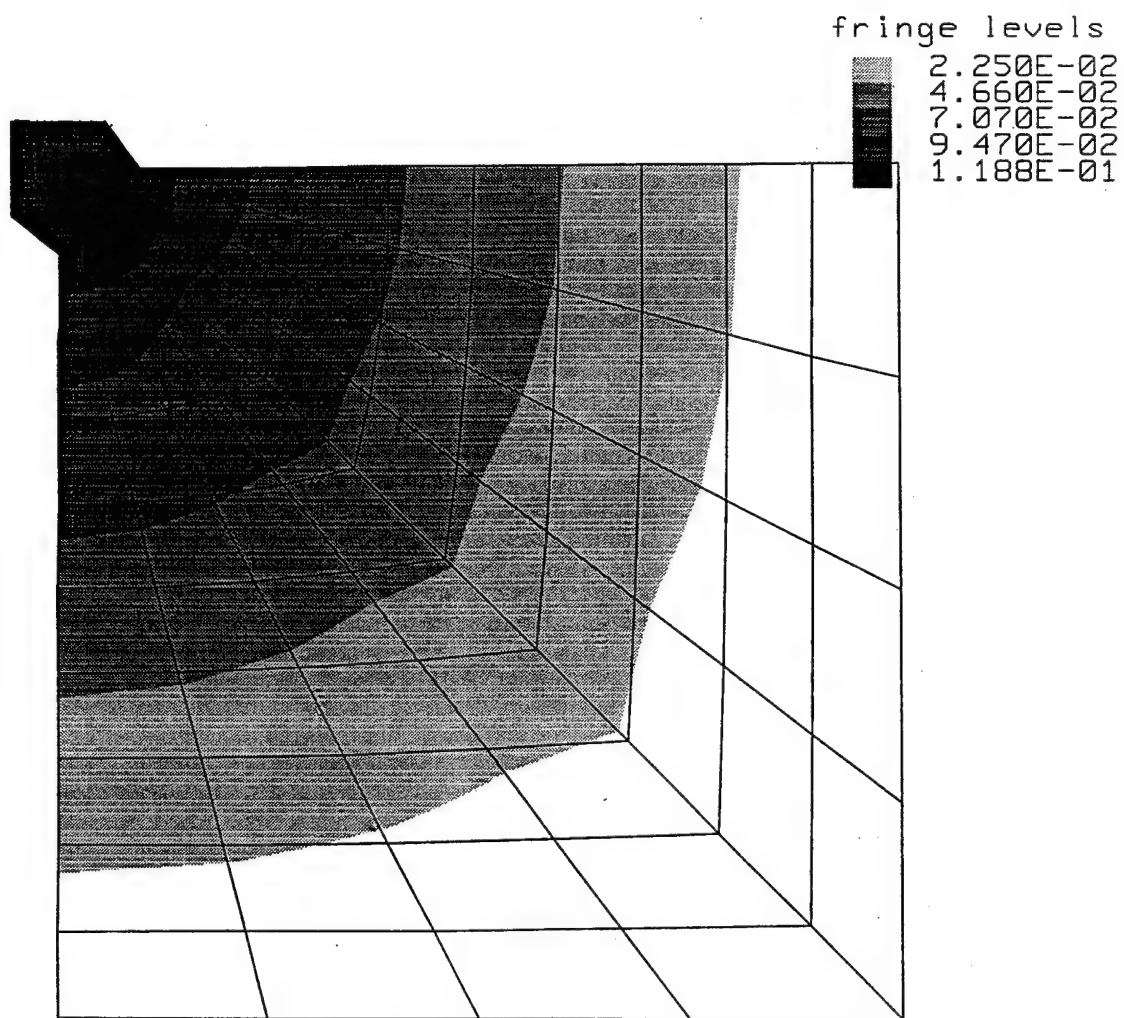
Figure 40. Fringes of z Displacement in Inches (Top View of Plate, t=.11400x10^{-2} s)

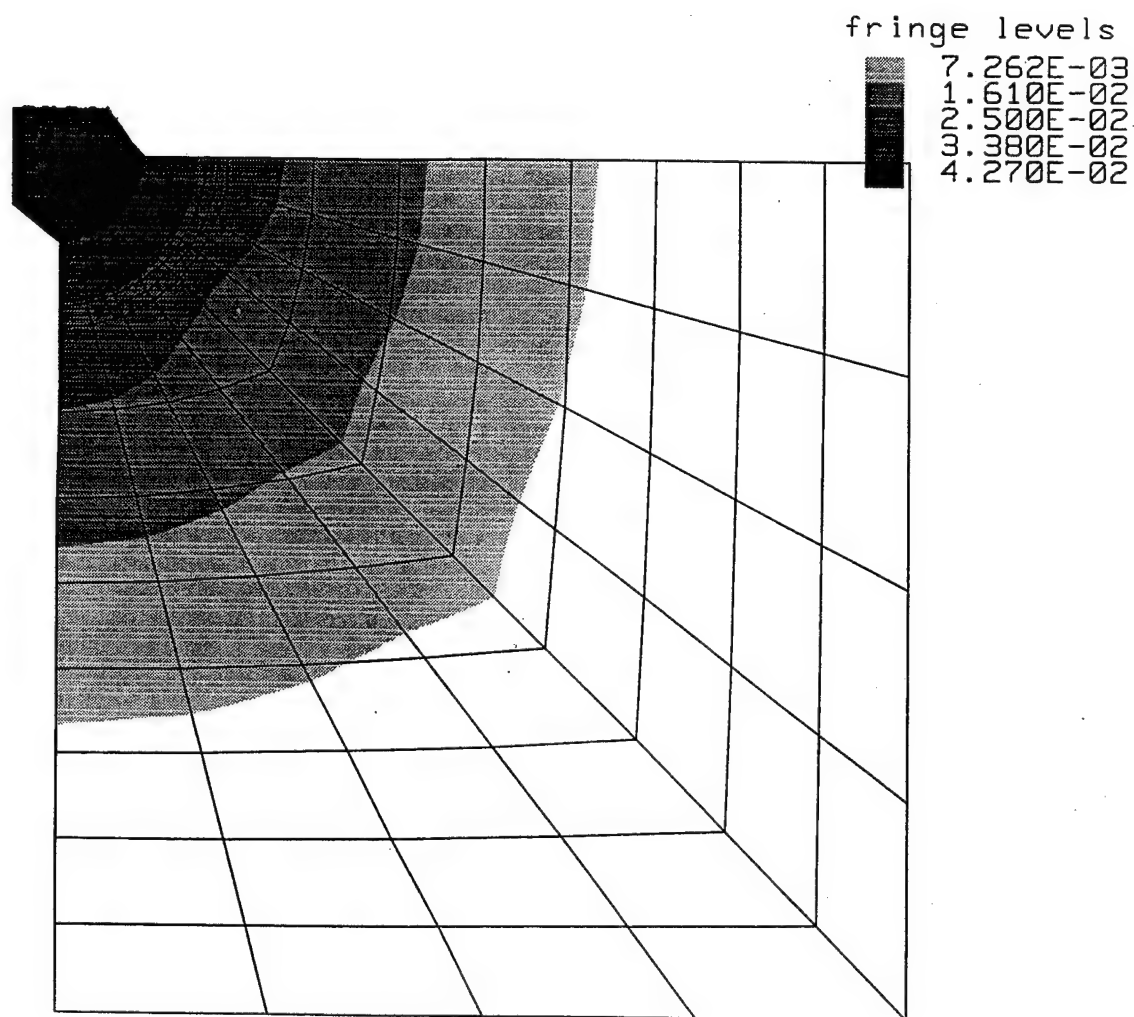fringe levels
2.840E-02
5.800E-02
8.760E-02
1.172E-01
1.468E-01
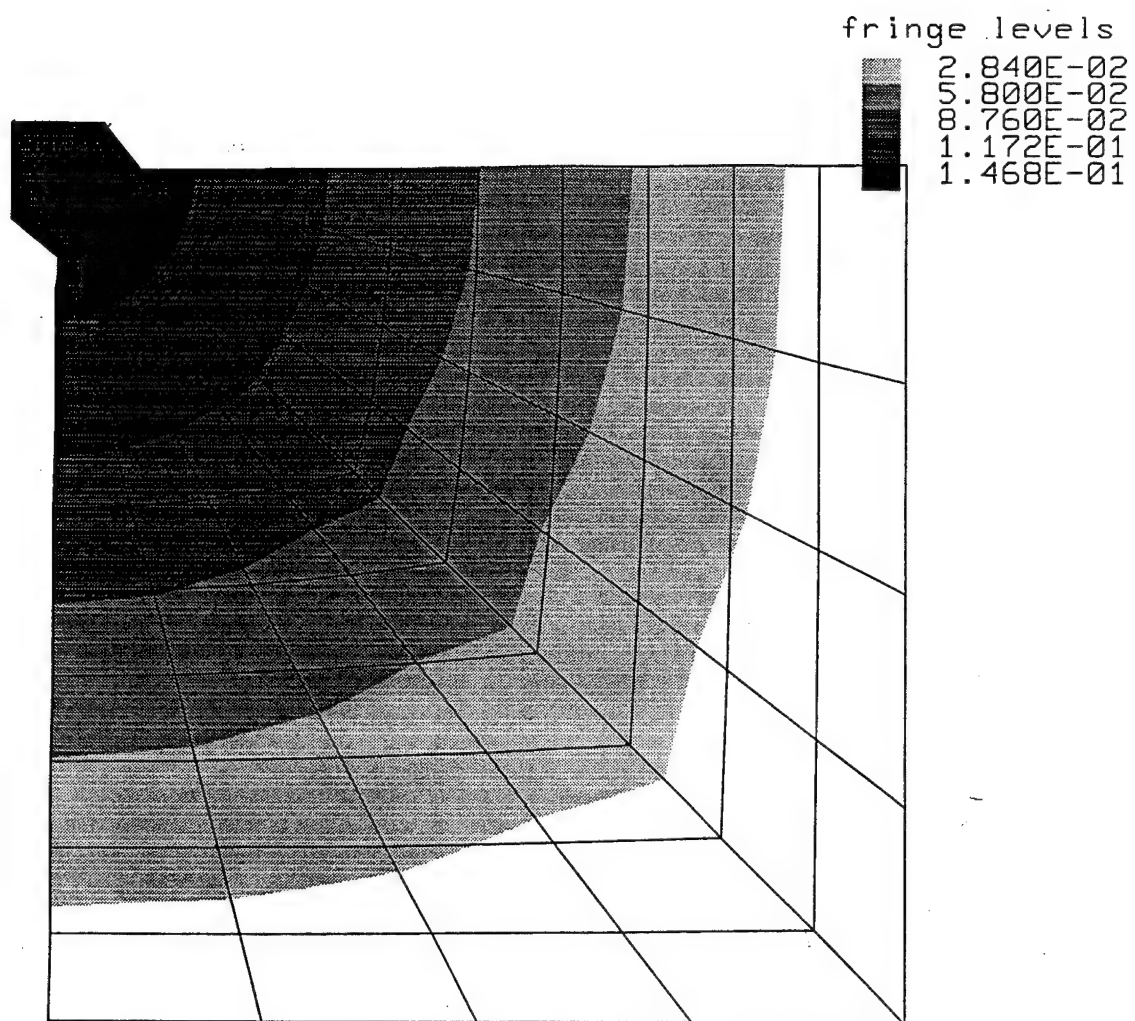
Figure 41. Fringes of z Displacement in Inches (Top View of Plate, t=0.17400x10^{-2} s)

64
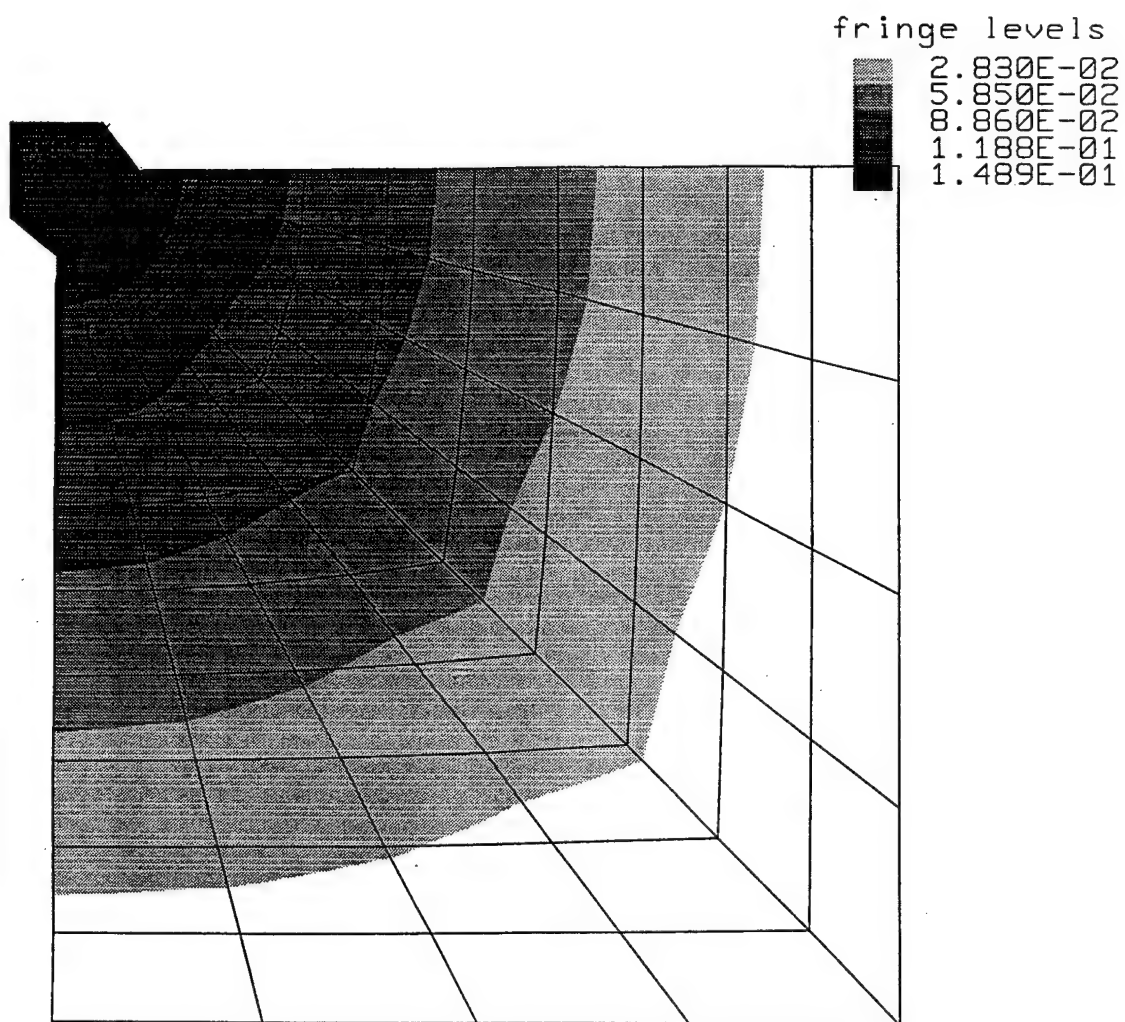
Figure 42. Fringes of z Displacement in Inches (Top View of Plate, t=0.19200x10^{-2} s)
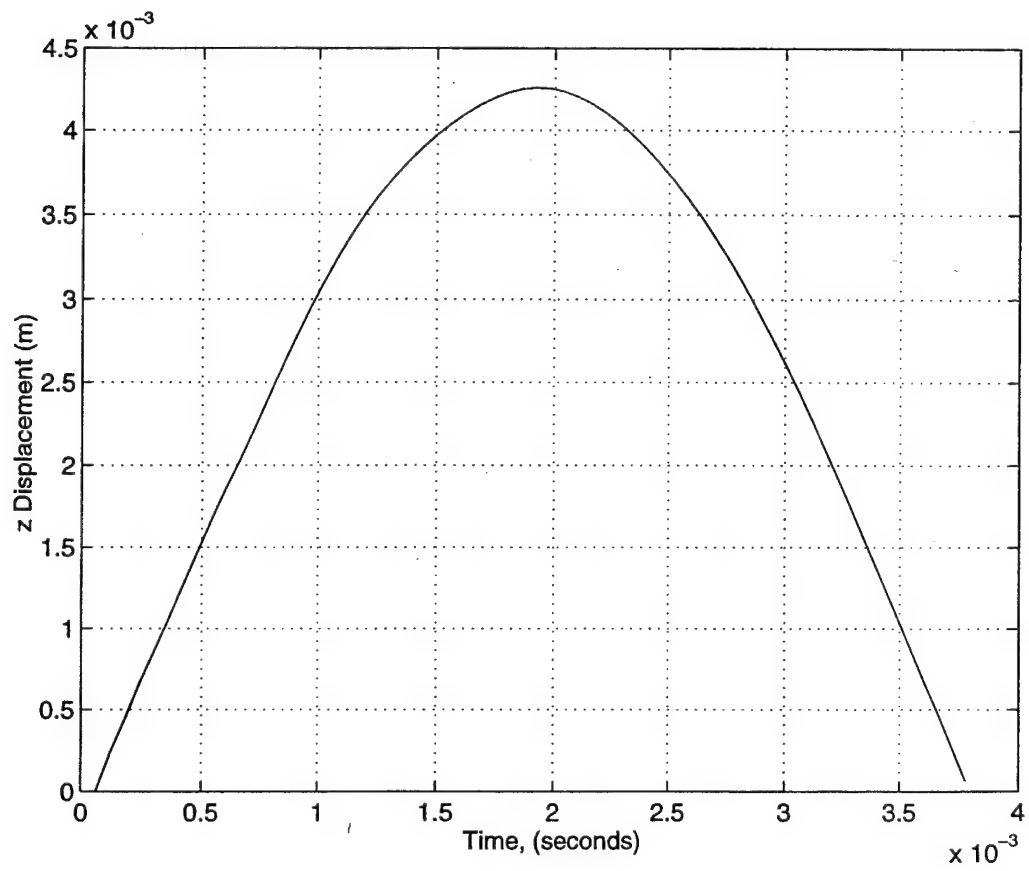
Figure 43. Midplate Deflection for No Delamination

66
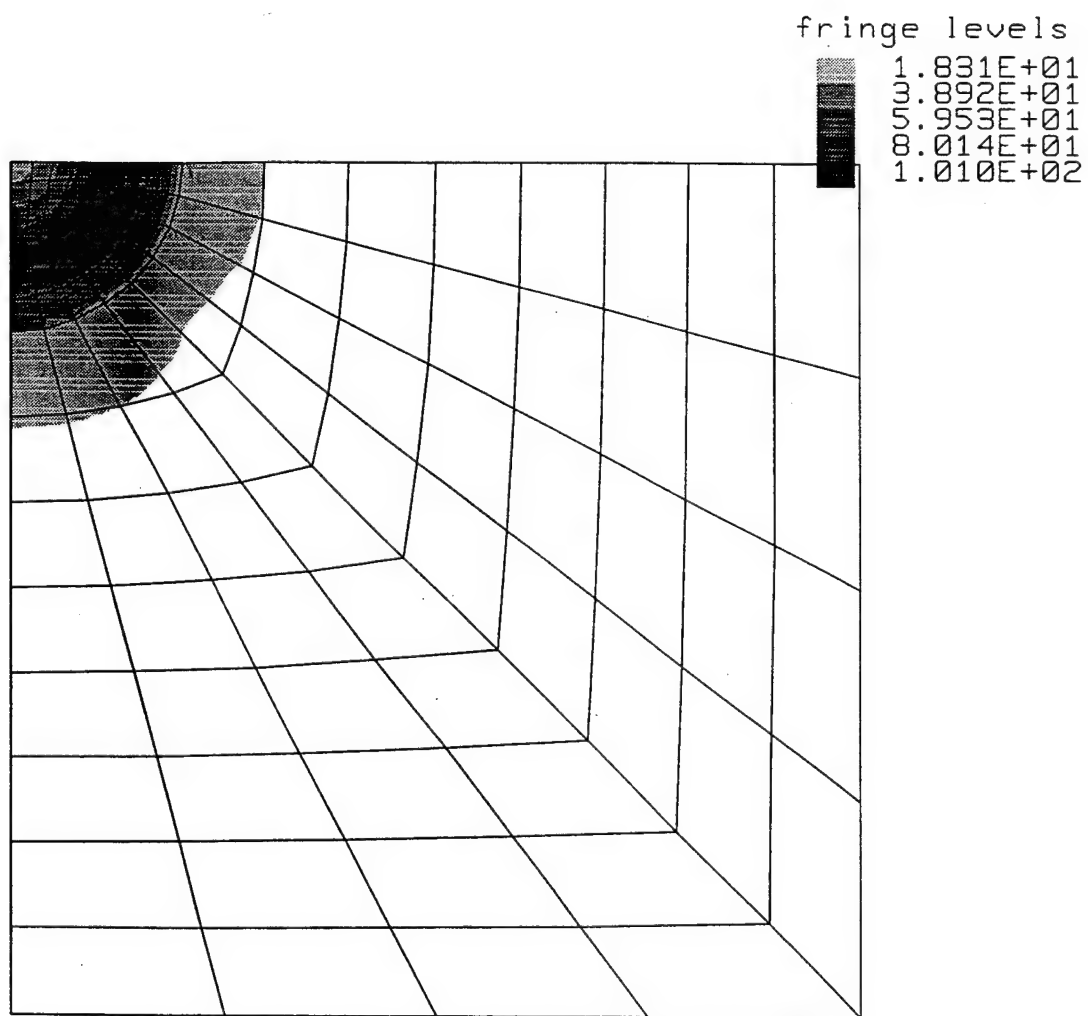
Figure 44. Fringes of Core τ_{max} in psi (Top View of Core, t=0.11995x10^{-3} s)
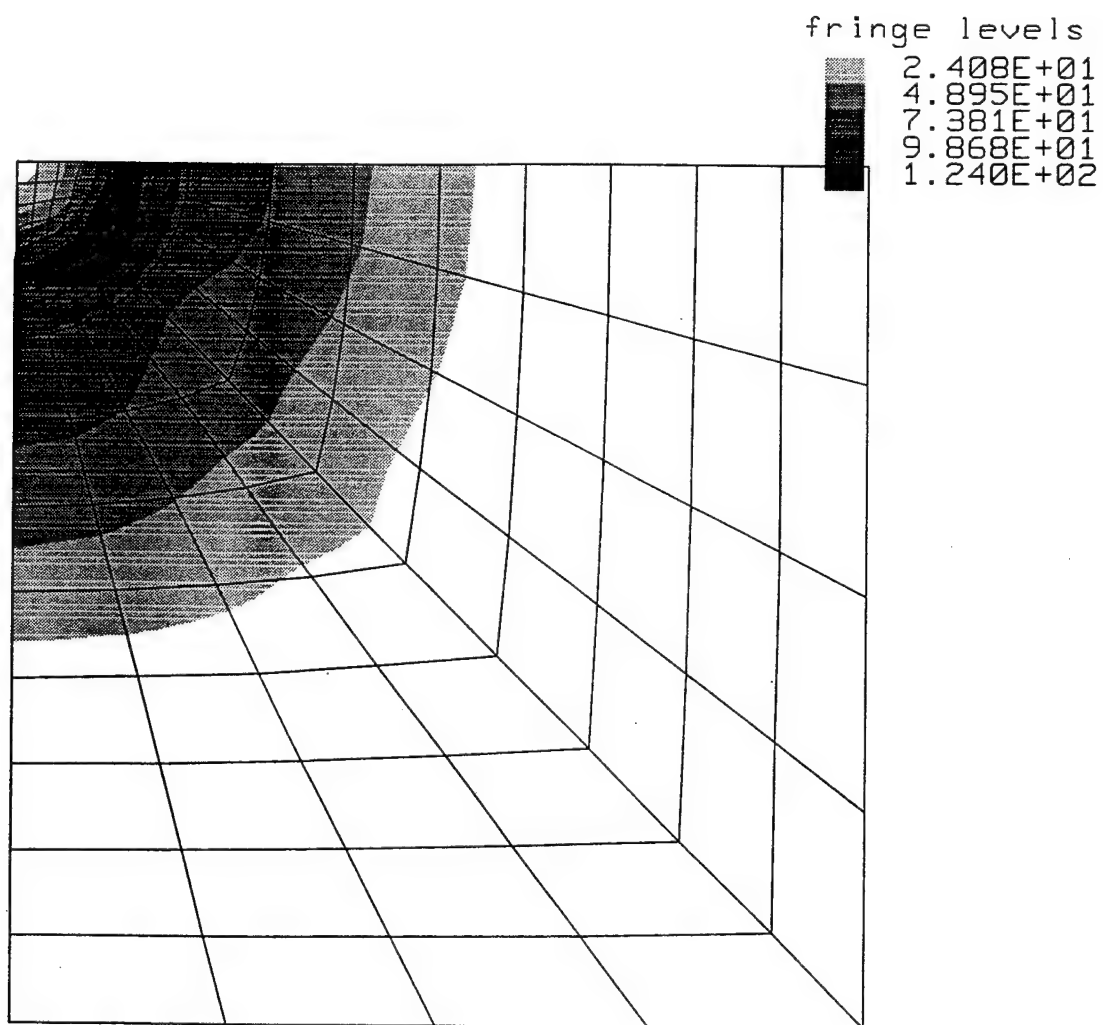
Figure 45. Fringes of Core τ_{max} in psi (Top View of Core, t=0.23999x10^{-3} s)

fringe levels
2.712E+01
5.578E+01
8.443E+01
1.130E+02
1.420E+02
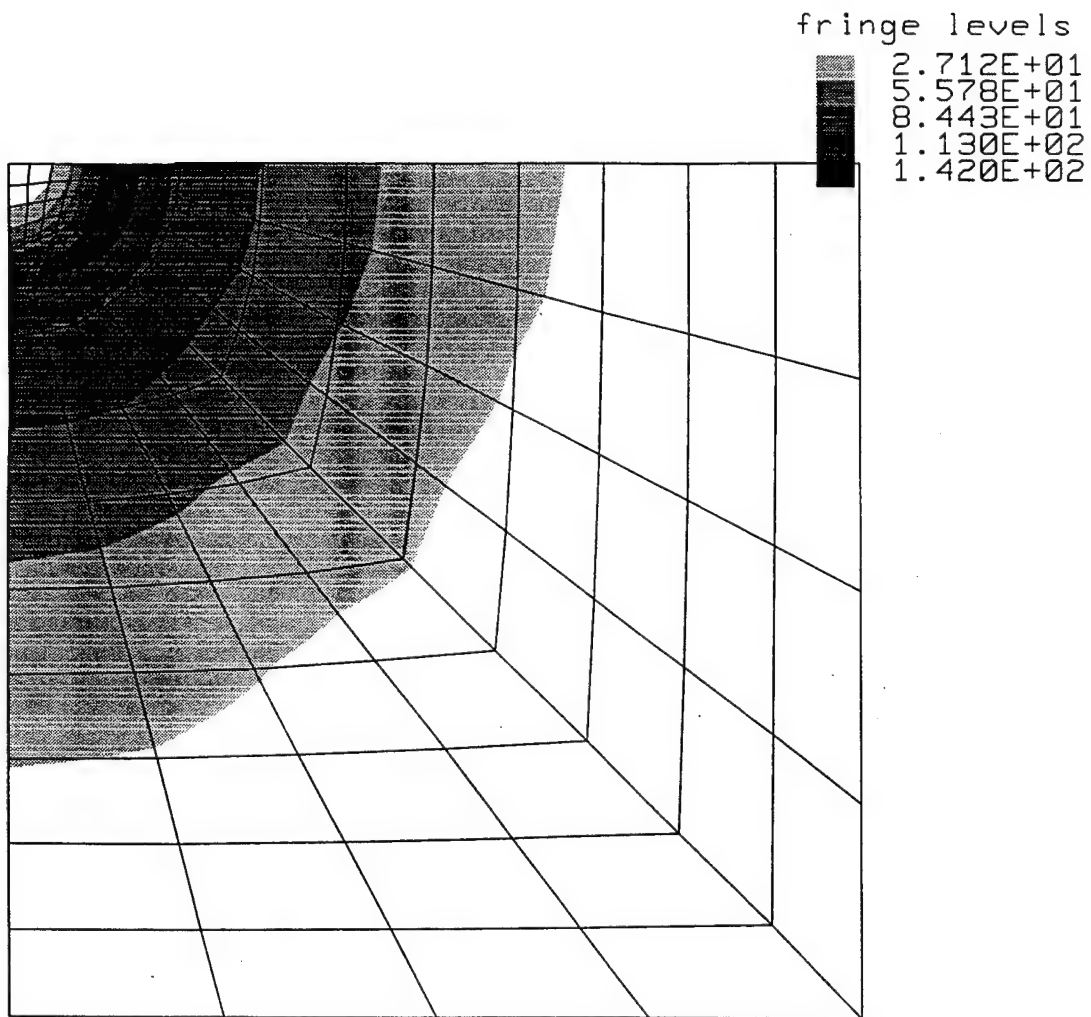
Figure 46. Fringes of Core τ_{max} in psi (Top View of Core, t=0.35996x10^{-3} s)
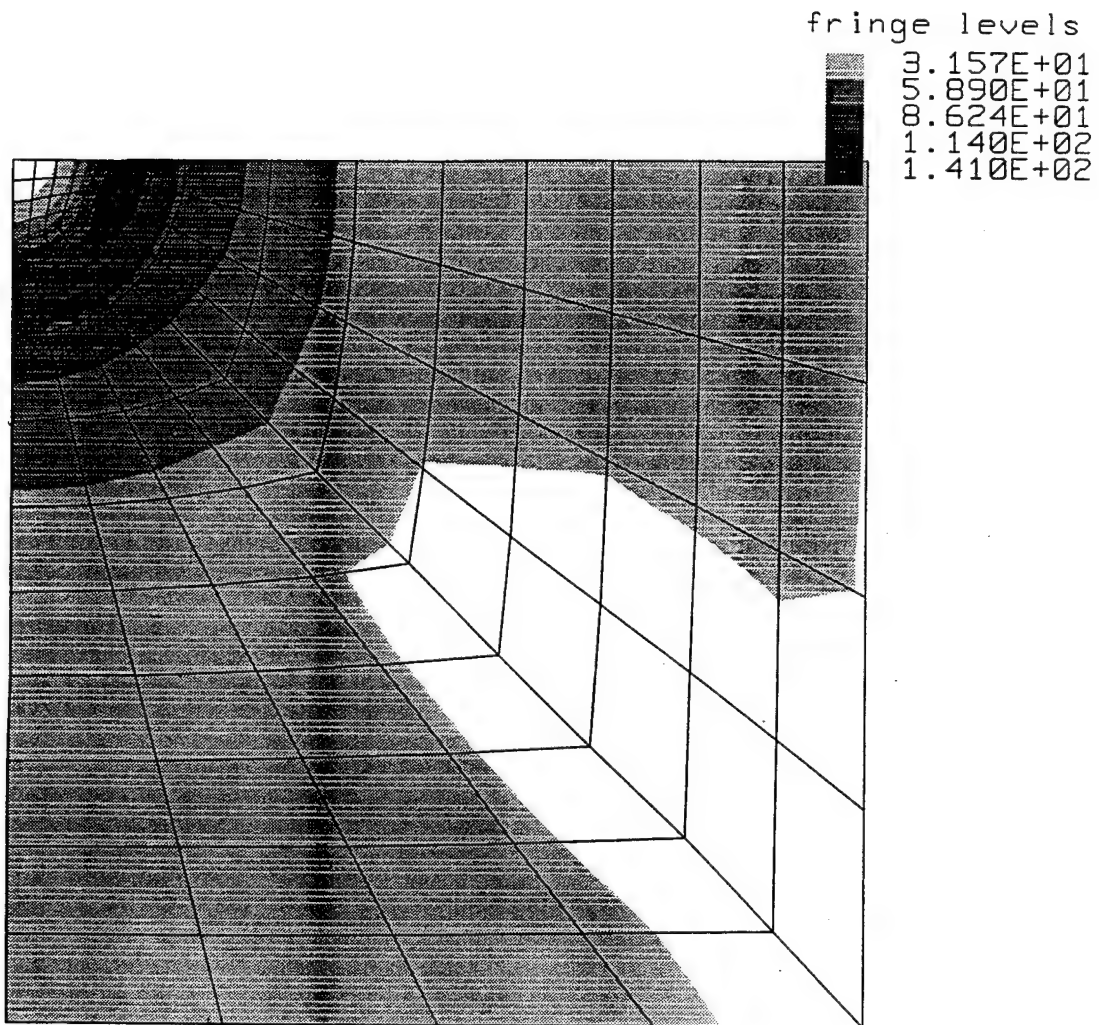
Figure 47. Fringes of Core τ_{max} in psi (Top View of Core, t=0.53998x10^{-3} s)

fringe levels
7.179E+01
1.390E+02
2.060E+02
2.740E+02
3.410E+02
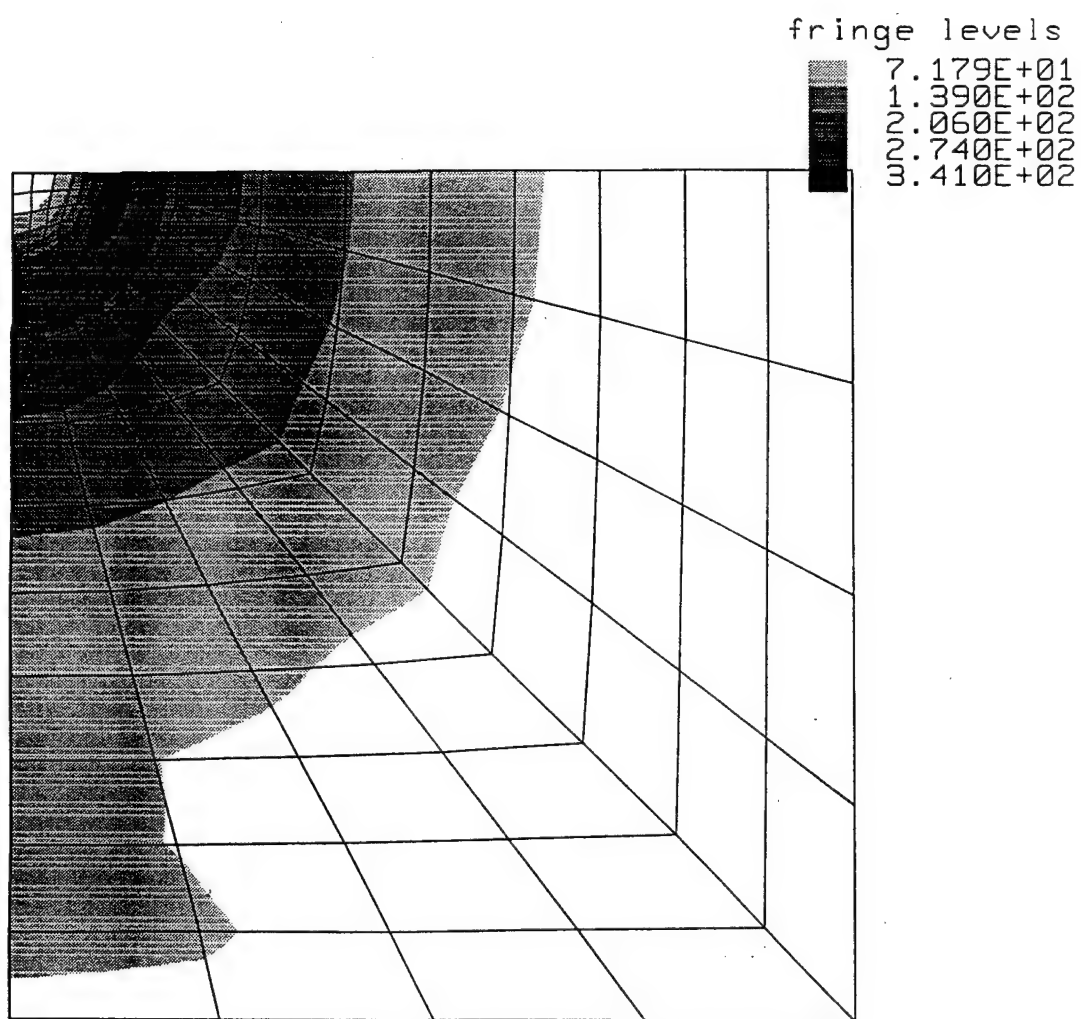
Figure 48. Fringes of Core τ_{max} in psi (Top View of Core, t=0.11400x10^{-2} s)

71

fringe levels
6.884E+01
1.380E+02
2.070E+02
2.760E+02
3.450E+02
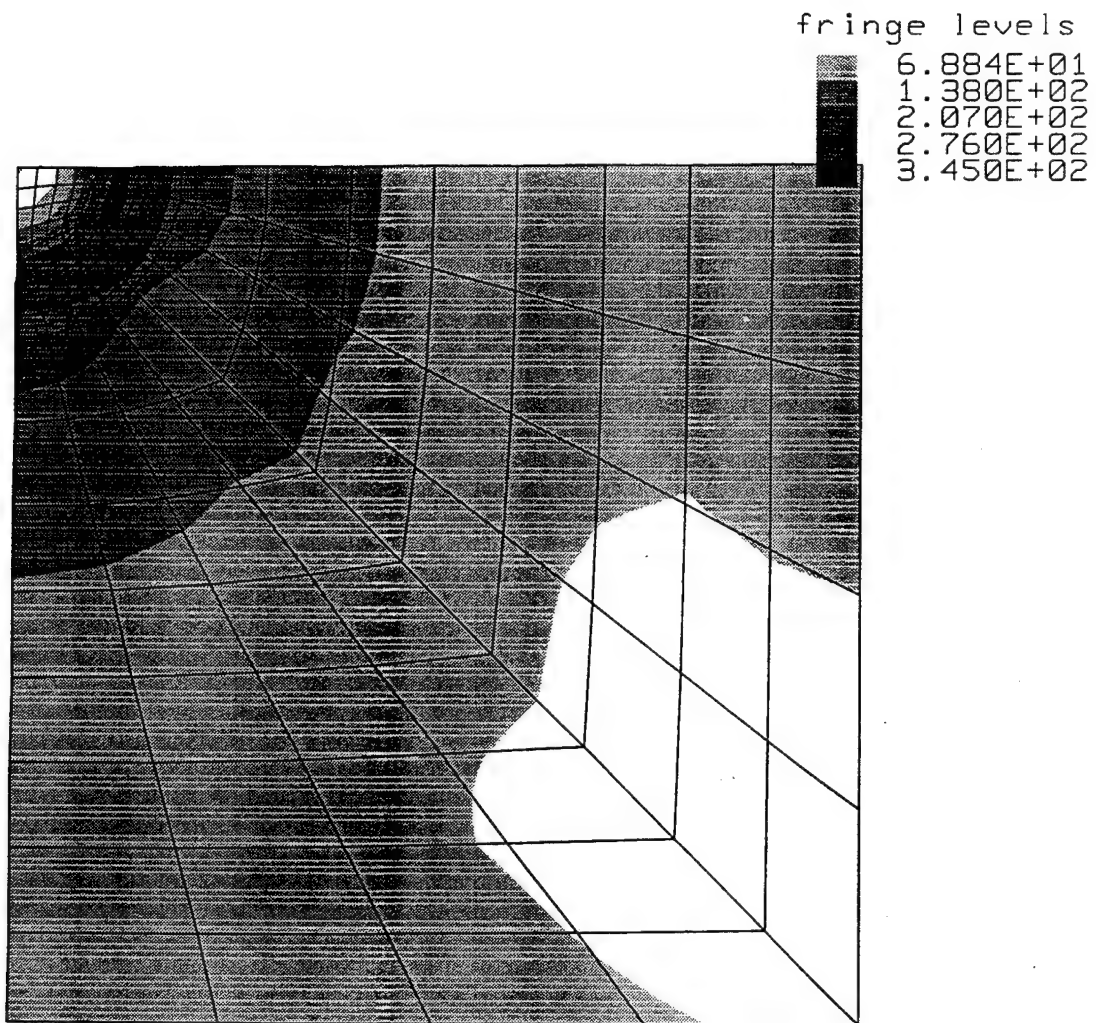
Figure 49. Fringes of Core τ_{max} in psi (Top View of Core, t=0.17400x10^{-2} s)

72

fringe levels
8.646E+01
1.700E+02
2.530E+02
3.360E+02
4.190E+02
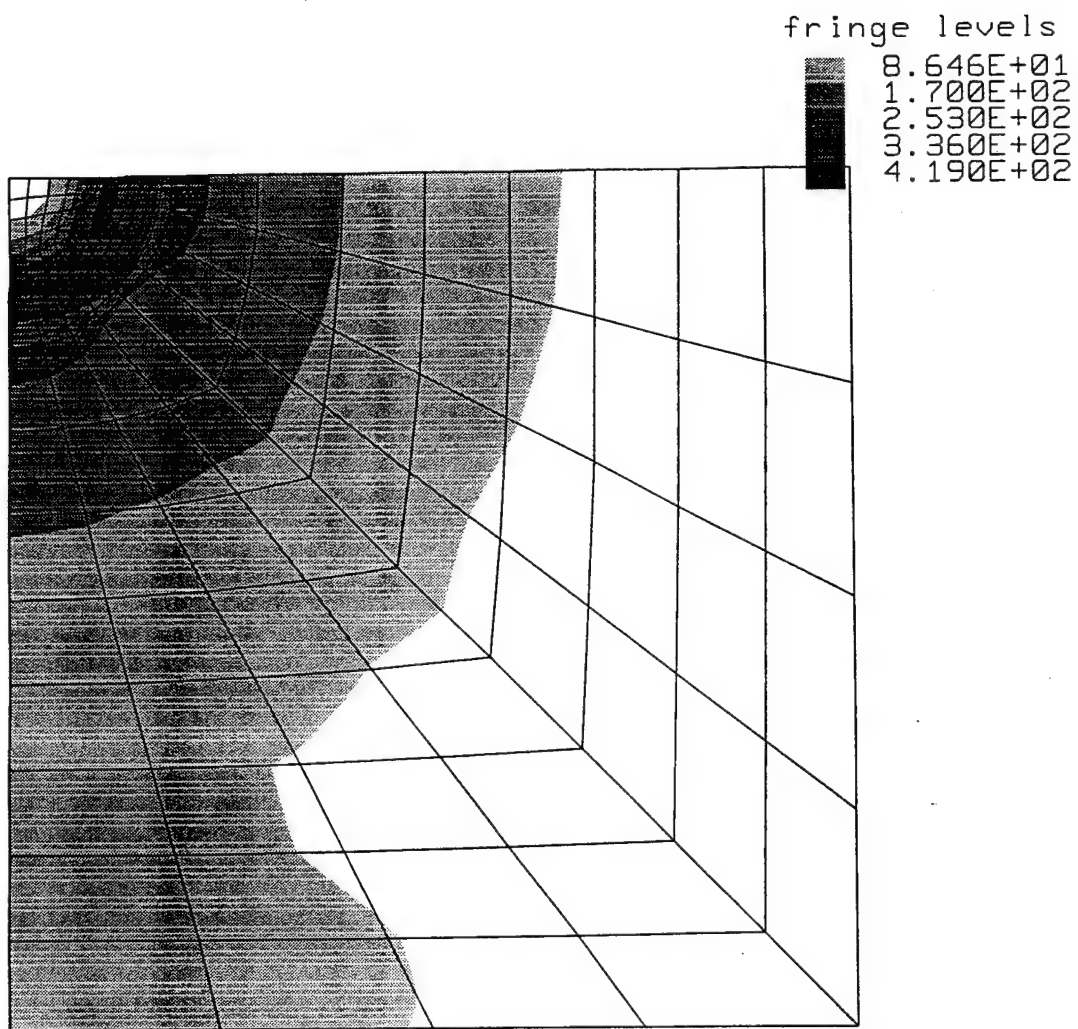
Figure 50. Fringes of Core τ_{max} in psi (Top View of Core, t=0.19800x10^{-2} s)
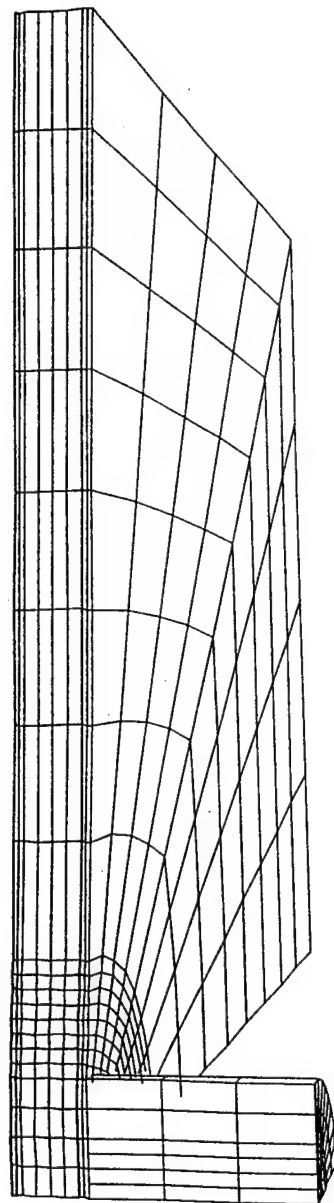
Figure 51. Plate/Impactor Orientation

74
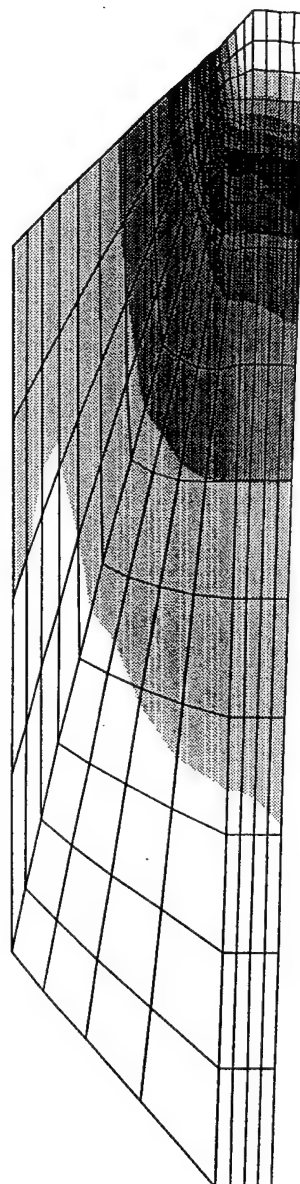
Figure 52. Fringes of Core Shear Stress (psi) at Maximum Deflection
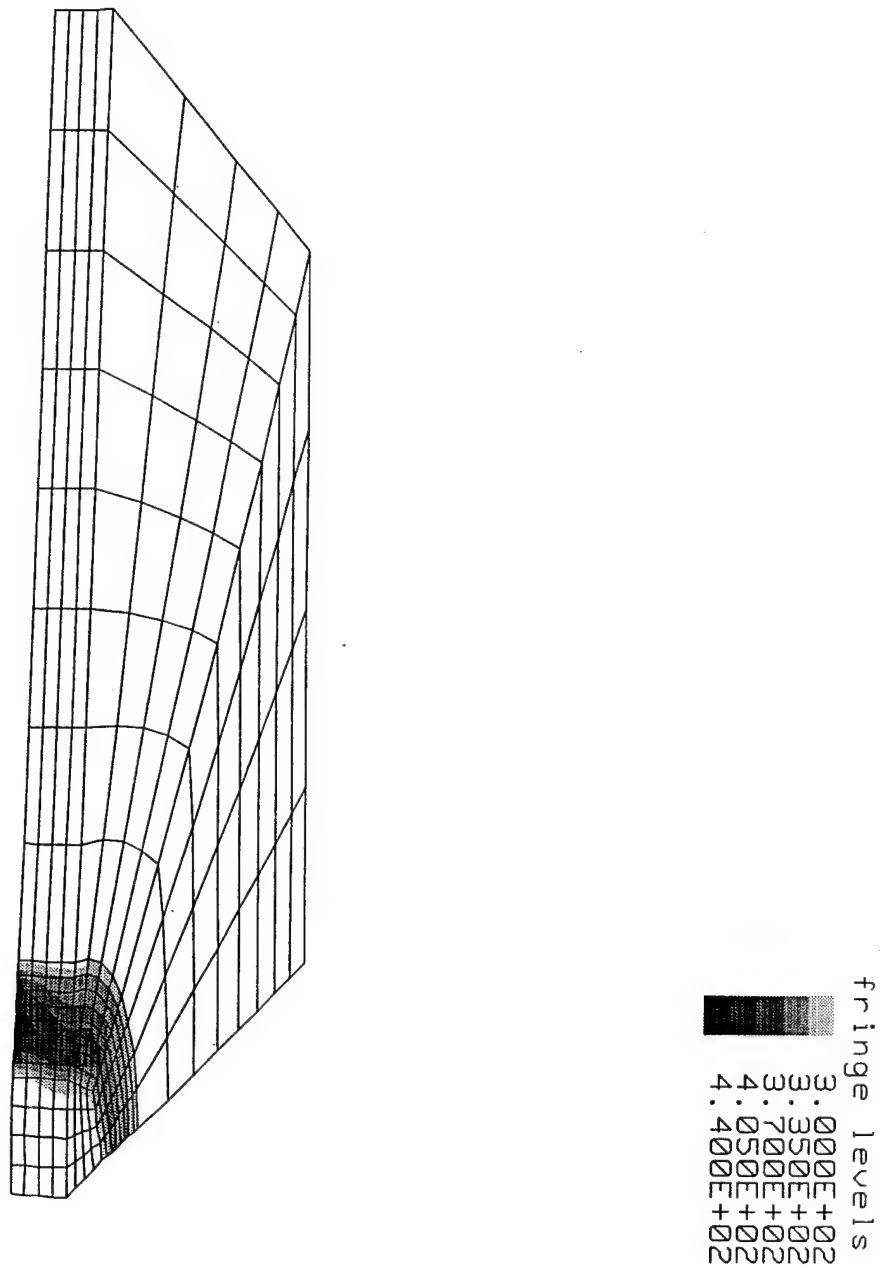
Figure 53. Fringes of Maximum Core Shear Stress (psi) at Maximum Deflection (narrow fringe scale)
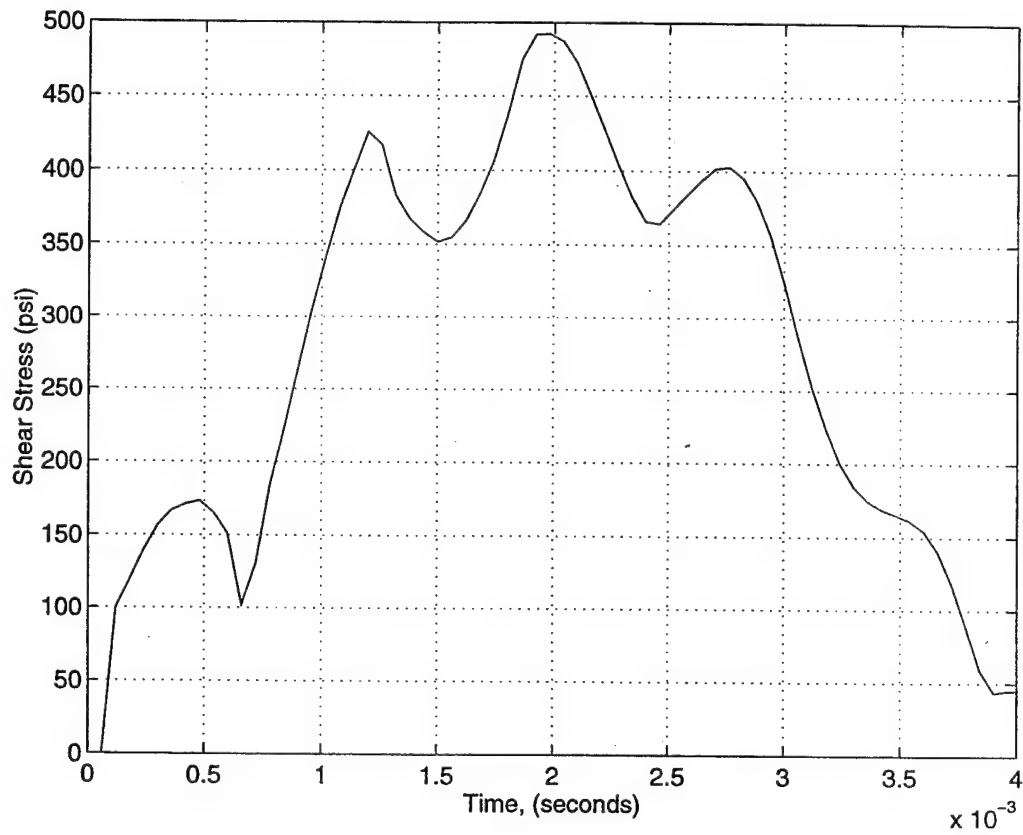
Figure 54. Maximum Radial Area Shear Stress for No Delamination

Table IV. Carbon Foam Plate Numerical Results

Delamination Radius (m) (in)	Maximum Deflection (m)(in)	τ_{max} (x10^3)	τ_{max} Location
None	0.004025 (0.1677)	0.4923	Radial Area
0.01016 (0.4)	0.004277 (0.1684)	0.4780	Radial Area
0.0127 (0.5)	0.004321 (0.1701)	0.4887	Radial Area
0.0245 (1.0)	0.004526 (0.1782)	0.6438	Delam Tip

Several points of importance are noteworthy from this data:

- Maximum deflection increased with the presence of a delamination. Furthermore, the larger the delamination, the greater the deflection. However, the change in magnitude of the deflection was quite small.

- As in the case of the delaminated beam, the presence of a small delamination (0.01016 m / 0.4 in or 0.0127 m / 0.5 in) lead to a decrease in the maximum shear stress. Increasing the radius of the delamination (0.0254 m / 1.0 in) caused a significant rise in the shear stress.

- Also as in the case of the delaminated beam, a large delamination caused a change of location in the core of the maximum attained shear stress. Rather than the radial area, the greatest shear stress occurred at the edge of the delamination, again illustrating the effect of crack length as a stress concentrator. Figure 55 shows a fringe plot of the maximum shear stress at the bottom of the core for a 0.0254 m (1.0 in) delamination at the time of maximum deflection. The ring of maximum stress corresponds to the delamination boundary.
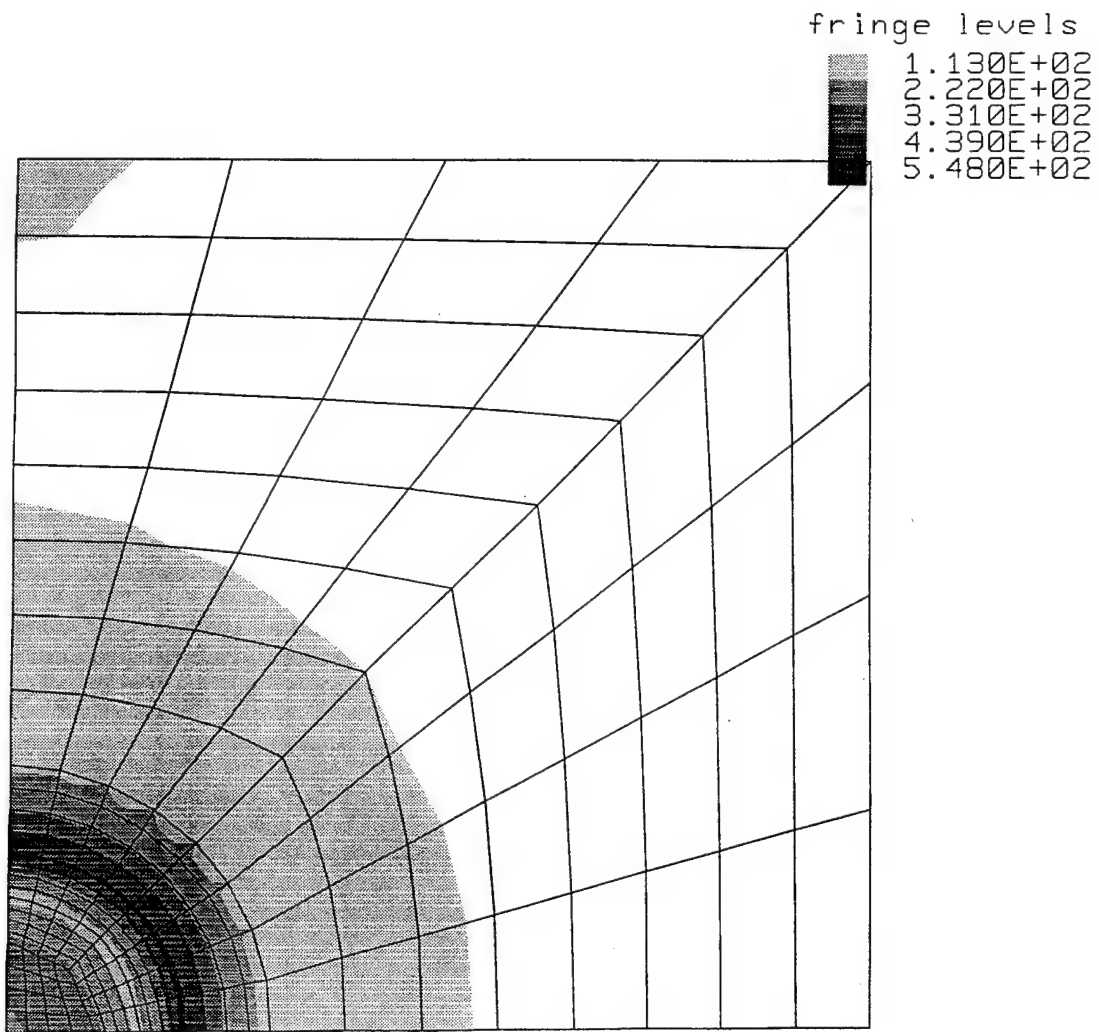
Figure 55. Fringes of Maximum Core Shear Stress in psi (Bottom View)

Delaminations in a sandwich composite are difficult to detect. In the analysis of the above data, it was hoped that evidence of a delamination would present itself in the deflection vs. time response. Specifically, it was hoped that delamination damage, particularly of a large radius, would yield a significant change in the maximum deflection recorded and thereby provide a relatively simple testing technique. Unfortunately, this was not the case. The increase in deflection of the 1.0 in delamination model was only 6% greater than that of the undelaminated model. Therefore, it appears that measuring displacement under load will not provide a good indication of the presence of a delamination.

In all the above delamination models (beam and plate), the effect of friction in the delamination areas was neglected (assumed to be zero). In reality, this is certainly not the case. A coefficient of friction, both static and dynamic, will exist between the core and the faceplate. To obtain a feel for the relative effect of this friction on the impact response, several models were run with values of the coefficients of friction equal to 0.1 and 0.2. Results are presented in Table V.

Table V. Carbon Foam Plate Coefficient of Friction Results

Delamination Radius (m) (in)	Coefficients of Friction	Maximum Deflection (in)	τ_{max} (x10³)
0.0127 (0.5)	0	0.004321 (0.1701)	0.4887
	0.1	0.004300 (0.1693)	0.4878
	0.2	0.004298 (0.1692)	0.4871
0.0254 (1.0)	0	0.004526 (0.1782)	0.6438
	0.1	0.004519 (0.1779)	0.6338
	0.2	0.004511 (0.1776)	0.6258

Observing the data in this table, it is clear that, as would be expected, maximum values of deflection and shear were lower in the presence of friction. However, the magnitude of the change was quite small. For a small delamination, the effect on both was approximately 0.5%. For a large delamination, the effect on maximum shear was larger, approximately 2.5% for a coefficient of friction of 0.2.

V. CONCLUSIONS

In this research, the impact response of three different types of sandwich construction were investigated: an unbalanced sandwich beam, a balanced sandwich beam, and a balanced sandwich plate. Although the types of construction varied, many characteristics of the responses and failure modes were similar.

The significant findings of this research were:

- In general, classical beam bending theory is not applicable in the analysis of sandwich beam response.

- Transverse shear and through-thickness deformations in a sandwich are quite significant. They allow the top and bottom surfaces of the sandwich to deform differently and appear to absorb some of the energy of impact.

- There appears to exist a threshold value of core shear modulus G_{yz} below which the non-impacted surface of a sandwich beam may enter a second mode bending configuration during impact.

- Core shear failure due to impact is likely to be asymmetric (occur on one side only).

- In the presence of a small delamination, the failure load of a sandwich beam increases. This is due to a drop in core shear stress caused by the short delamination crack.

- In the presence of a large delamination, the location of maximum core shear stress, and therefore the probable location of failure, shifts from the quarter area in a beam (radial area for a plate) to the delamination boundary.

- The presence of a delamination appears to not significantly change the magnitude of the deflection vs. time response. Therefore, it seems that detecting a delamination from this data would be difficult.

- The effect of friction in the delamination area is a very small factor in the dynamic response of the composite.

83

There is still a significant amount of work and research that is required to be done in order to fully understand the dynamic response and failure of a sandwich composite subject to low velocity impact. This applies to both the areas of experimental testing and computer modeling.

In the realm of dynamic response, testing with fully instrumented beam surfaces could yield a better understanding of why portions of the bottom surface appear to enter compression rather than remain in tension. Additionally, with regard to modeling, the simulation of a honeycomb core is a point of interest. In this study, the honeycomb's material properties were smeared, i.e., regarded as continuous. In actuality, this is certainly not the case. Honeycomb is full of void areas and is not continuous. Modeling honeycomb in a different manner could have an appreciable influence on the predicted response

This research investigated only the initiation of failure in a sandwich composite. It did not attempt to develop or verify any failure criterion. Future work should incorporate doing this, as well as continuing on to model the complete failure process.

LIST OF REFERENCES

1. Fuller, L. B., (1994) *Damage and Compressive Failure of Unbalanced Sandwich Composite Panels Subject to Low Velocity Impact,* Master's Thesis, Naval Postgraduate School, Monterey, California.

2. Clawson, L. A., (1995) *Experimental Study of a Delaminated Sandwich Composite Subject to Impact and/or Compressive Loading,* Master's Thesis, Naval Postgraduate School, Monterey, California.

3. Nemes, J. A., and Simmonds, K. E., (1992) "Low-Velocity Impact Response of Foam-Core Sandwich Composites," *Journal of Composite Materials*, 26, 4.

4. Lee, L. J., Huang, K. Y., and Fann, Y. J., (1993) "Dynamic Responses of Composite Sandwich Plate Impacted by a Rigid Ball," *Journal of Composite Materials*, 27, 13.

5. Sjoblom, P. O., Hartness, J. T., and Cordell, T. M., (1988) "On Low-Velocity Impact Testing of Composite Materials," *Journal of Composite Materials*, 22, January.

6. Wu, E. and Shyu, K., (1993) "Response of Composite Laminates to Contact Loads and Relationship to Low-Velocity Impact," *Journal of Composite Materials*, 27, 15.

INITIAL DISTRIBUTION LIST

<div align="right">No. Copies</div>

1. Defense Technical Information Center 2
   8725 John J. Kingman Rd. STE 0944
   Ft. Belvoir, VA 22060-6218

2. Library, Code 13 2
   Naval Postgraduate School
   Monterey, California 93943-5101

3. Professor Y. W. Kwon, Code ME/Kw 2
   Department of Mechanical Engineering
   Naval Postgraduate School
   Monterey, California 93943-5000

4. Department Chairman, Code ME/Kk 1
   Department of Mechanical Engineering
   Naval Postgraduate School
   Monterey, California 93943-5000

5. Naval Engineering Curricular Office, Code 34 1
   700 Dyer Rd, Rm 115
   Naval Postgraduate School
   Monterey, California 93943-5000

6. Dr. Vincent J. Castelli 1
   Naval Surface Warfare Center, Carderock Div.
   Composites and Resins Branch, Code 644
   Annapolis, Maryland 21402-5067

7. Mr. Paul Coffin 1
   Naval Surface Warfare Center, Carderock Div.
   Composites and Resins Branch, Code 644
   Annapolis, Maryland 21402-5067

8. LCDR Gerald W. Wojcik 1
   504 Earl Ave.
   New Kensington, Pennsylvania 15068